

Passive Array Correlation-Based Imaging in a Random Waveguide

Habib Ammari*

Josselin Garnier[†]Wenjia Jing[‡]

October 18, 2018

Abstract

We consider reflector imaging in a weakly random waveguide. We address the situation in which the source is farther from the reflector to be imaged than the energy equipartition distance, but the receiver array is closer to the reflector to be imaged than the energy equipartition distance. As a consequence, the reflector is illuminated by a partially coherent field and the signals recorded by the receiver array are noisy. This paper shows that migration of the recorded signals cannot give a good image, but an appropriate migration of the cross correlations of the recorded signals can give a very good image. The resolution and stability analysis of this original functional shows that the reflector can be localized with an accuracy of the order of the wavelength even when the receiver array has small aperture, and that broadband sources are necessary to ensure statistical stability, whatever the aperture of the array.

1 Introduction

Sensor array imaging in a scattering medium is limited because coherent signals recorded at the source-receiver array and coming from a reflector to be imaged are dominated by incoherent signals coming from multiple scattering by the medium. For instance, in a randomly perturbed waveguide, it is known that the field becomes completely incoherent when the propagation distance becomes larger than the equipartition distance, which corresponds to the distance beyond which the source energy has been shared equally among all the propagating modes [10, Chapter 20]. As we will see, if the distance between the source-receiver array and the reflector is larger than the equipartition distance, then classical migration of the signals recorded at the array cannot give a good image.

Sources can be expensive or difficult to implement but receivers can be cheap and easy to implement, so an imaging problem in which there are a few sources (all of them being far from the reflector) and many receivers (some of them being close to the reflector) is

*Département de Mathématiques et Applications, Ecole Normale Supérieure, 45 Rue d'Ulm, 75230 Paris Cedex 05, France. Email: habib.ammari@ens.fr

[†]Laboratoire de Probabilités et Modèles Aléatoires & Laboratoire Jacques-Louis Lions, Université Paris VII, 75205 Paris Cedex 13, France. Email: garnier@math.univ-paris-diderot.fr

[‡]Département de Mathématiques et Applications, Ecole Normale Supérieure, 45 Rue d'Ulm, 75230 Paris Cedex 05, France. Email: wjing@dma.ens.fr

of theoretical and practical interest. If there is a unique source far from the reflector (farther than the equipartition distance) and if the receiver array is close to the reflector (closer than the equipartition distance), then classical migration of the recorded signals fails again. This was shown in various contexts and we will show it again in the waveguide geometry. However, in such a situation, another kind of migration can be used: from the work devoted to coherent interferometry imaging [4, 5, 6, 7, 8] and ambient noise imaging [9, 12, 16, 17, 18], it is known that migration of cross correlations of noisy signals can be more stable than migration of the signals themselves. The migration of cross correlations of noisy signals recorded by auxiliary passive arrays was proposed by [3] in geophysical contexts and analyzed recently in randomly scattering open media in [14], and we would like to address the same problem in the waveguide geometry. Indeed the number of propagating modes is finite in the waveguide geometry so that the statistical behavior of partially coherent fields in random waveguides is very different from the open medium case [11, 10]. In our paper, we show that, if a receiver array can be placed close to the reflector to be imaged, then the cross correlations of the incoherent signals on this array can be used to image the reflector. We will give a detailed resolution and stability analysis. We will show that the statistical stability requires a broadband source and that good resolution and stability properties do not require the receiver array to span the whole cross section of the waveguide, which is an effect specific to the waveguide geometry.

The paper is organized as follows. In section 2, we review the mathematical background of the imaging problem in a random waveguide. In section 3 we describe and analyze the classical migration functional using the recorded signals and show that it cannot give a good image when the propagation distance is beyond the energy equipartition distance. In section 4, we introduce the correlation-based imaging functional; it has two versions which correspond to the time-harmonic case and the broadband case. In section 5, we analyze the resolution of the proposed imaging functionals. Detailed analyses are provided for full aperture and limited aperture arrays. These results are based on the statistical average of the imaging functionals. The variances of these functionals are very important as well because they determine the statistical stability of the imaging functionals. In section 6, we study the variances of the imaging functionals. Some concluding remarks are listed at the end of the paper.

2 Mathematical Formulation of the Imaging Problem

2.1 The ideal waveguide

We consider linear scalar (acoustic) waves propagating in a two-dimensional space. The governing equation is

$$\Delta p(t, \mathbf{x}) - \frac{1}{c_0^2} \frac{\partial^2 p}{\partial t^2}(t, \mathbf{x}) = F(t, \mathbf{x}). \quad (2.1)$$

Here p is the scalar field (acoustic pressure); c_0 is the speed of propagation in the medium (sound speed); $F(t, \mathbf{x})$ models the forcing term. We consider a waveguide geometry, and we decompose the spatial variable \mathbf{x} as (x, z) . That is, $z \in \mathbb{R}$ is along the axis of the waveguide while $x \in \mathcal{D}$ denotes the transverse coordinate, and $\mathcal{D} = (0, a)$ is the transverse section of

the waveguide. We assume that the forcing term is localized in the plane $z = 0$:

$$F(t, \mathbf{x}) = f(t)\delta(\mathbf{x} - \mathbf{x}_{\text{source}}), \quad (2.2)$$

where $\mathbf{x}_{\text{source}} = (x_s, 0)$ for some $x_s \in \mathcal{D}$. We assume that the medium is quiescent before the pulse emission, that is

$$p(t, \mathbf{x}) = 0, \quad t \ll 0. \quad (2.3)$$

We consider Dirichlet boundary conditions at the boundary of the waveguide:

$$p(t, \mathbf{x}) = 0, \quad \mathbf{x} \in \partial\mathcal{D} \times \mathbb{R} = \{0, a\} \times \mathbb{R}. \quad (2.4)$$

Using the Fourier method, the scalar field can be written as a superposition of waveguide modes. A waveguide mode is a time-harmonic wave of the form $\hat{p}(\omega, \mathbf{x})e^{-i\omega t}$ with frequency ω , where \hat{p} satisfies the time-harmonic form of the wave equation (2.1) without a source term:

$$\partial_z^2 \hat{p}(\omega, x, z) + \Delta_{\perp} \hat{p}(\omega, x, z) + k^2(\omega) \hat{p}(\omega, x, z) = 0. \quad (2.5)$$

Here, $\Delta_{\perp} = \partial_x^2$ is the transverse Laplace operator in the transverse section \mathcal{D} with Dirichlet boundary conditions; $k(\omega) = \omega/c_0$ is the homogeneous wavenumber. Consequently, (2.5) can be solved using the eigenmodes of Δ_{\perp} , that is, using the orthonormal basis $\{\phi_j(x)\}_{j=1,2,\dots}$ of $L^2(\mathcal{D})$ given by

$$-\Delta_{\perp} \phi_j(x) = \lambda_j \phi_j(x), \quad x \in \mathcal{D}. \quad (2.6)$$

The eigenvalues are simple, satisfying $0 < \lambda_1 < \lambda_2 < \dots$. The eigenvalues and eigenvectors are given by

$$\phi_j(x) = \frac{\sqrt{2}}{\sqrt{a}} \sin\left(\frac{\pi j x}{a}\right), \quad \lambda_j = \frac{\pi^2 j^2}{a^2}. \quad (2.7)$$

Using the method of separation of variables on (2.5), we see that the waveguide mode $\hat{p}(\omega, x, z)$ can be further written as superposition of $\hat{p}_j(\omega, x, z) = \phi_j(x)e^{\pm i\beta_j(\omega)z}$, where

$$\beta_j^2(\omega) = k^2(\omega) - \lambda_j. \quad (2.8)$$

For a given frequency ω , there exists a unique integer $N(\omega)$ such that $\lambda_{N(\omega)} \leq k^2(\omega) < \lambda_{N(\omega)+1}$:

$$N(\omega) = \left\lfloor \frac{\omega a}{\pi c_0} \right\rfloor. \quad (2.9)$$

Here and in the sequel, $\lfloor b \rfloor$ means the integer part of a real number b . The modes $\{\hat{p}_j(\omega, x, z) = \phi_j(x)e^{\pm i\beta_j(\omega)z}\}_{j=1,\dots,N(\omega)}$ are propagating waveguide modes and $\{\beta_j(\omega)\}_{j=1,\dots,N(\omega)}$ are called the modal wavenumbers. On the other hand, $\{\hat{p}_j(\omega, x, z) = \phi_j(x)e^{\pm |\beta_j(\omega)|z}\}_{j>N(\omega)}$ are evanescent modes because they decay as z goes to $\mp\infty$.

2.2 The randomly perturbed waveguide

From now on we assume that the waveguide is randomly perturbed and the scalar field satisfies the perturbed wave equation

$$\Delta p(t, \mathbf{x}) - \frac{1}{c^2(\mathbf{x})} \frac{\partial^2 p}{\partial t^2}(t, \mathbf{x}) = F(t, \mathbf{x}), \quad (2.10)$$

where $c(\mathbf{x})$ is the randomly heterogeneous speed of propagation of the medium. We consider the case where the typical amplitude of the fluctuations of the speed of propagation is small, which we call the weakly random regime. When the correlation length of the fluctuations is of the same order as the typical wavelength the interactions between the waves and the random medium become nontrivial. Due to the small amplitude of the fluctuations, however, the effect of the interaction becomes important only after a long propagating distance.

More exactly we assume that a randomly heterogeneous section in $z \in [0, \tilde{L}_0]$ is sandwiched in between two homogeneous waveguides: The speed of propagation is of the form

$$\frac{1}{c^2(x, z)} = \begin{cases} \frac{1}{c_0^2}(1 + \varepsilon\nu(x, z)) & \text{if } (x, z) \in [0, a] \times [0, \tilde{L}_0], \\ \frac{1}{c_0^2} & \text{otherwise} \end{cases} \quad (2.11)$$

Here, ν is a mean-zero, stationary and ergodic random processes with respect to the axis coordinate z . It is assumed to satisfy strong mixing conditions in z . The relative amplitude of the fluctuations of the speed of propagation is denoted by ε . We assume that the correlation length of the random perturbation is of the same order as the typical wavelength $\lambda(\omega_0) = 2\pi c_0/\omega_0 = 2\pi/k(\omega_0)$, for ω_0 the central frequency of the source. We assume that the propagation distance \tilde{L}_0 is much larger than the typical wavelength. We will see that the interesting regime is when the ratio λ/\tilde{L}_0 is of order ε^2 , so we introduce the normalized propagation distance L_0 :

$$\tilde{L}_0 = \frac{L_0}{\varepsilon^2}.$$

In this regime the cumulative effects of the interaction of the scalar wave with the small fluctuations of the speed of propagation become of order one.

For a fixed frequency ω , the Fourier transformed scalar field $\hat{p}(\omega, x, z)$ defined by

$$\hat{p}(\omega, x, z) = \int p(t, x, z) e^{i\omega t} dt$$

satisfies the equation

$$\partial_z^2 \hat{p}(\omega, x, z) + \Delta_{\perp} \hat{p}(\omega, x, z) + k^2(\omega)[1 + \varepsilon\nu(x, z)]\hat{p}(\omega, x, z) = \hat{f}(\omega)\delta(x - x_s)\delta(z). \quad (2.12)$$

To solve this equation, we make the following two simplifications that are justified in [10, Chapter 20] or [11].

Ignoring the evanescent modes. First, we only consider the propagating modes:

$$\hat{p}(\omega, x, z) = \sum_{j=1}^{N(\omega)} \phi_j(x) \hat{p}_j(\omega, z). \quad (2.13)$$

This is valid because we are mainly concerned with the scalar field for $z \gg 1$ and the evanescent modes decay exponentially fast. Furthermore, we parameterize the complex mode amplitude $\hat{p}_j(\omega, z)$ by the amplitudes of its right- and left-going components. Let $\hat{a}_j(\omega, z)$ and $\hat{b}_j(\omega, z)$ be the amplitudes of these components, defined by

$$\hat{p}_j = \frac{1}{\sqrt{\beta_j}} \left(\hat{a}_j e^{i\beta_j z} + \hat{b}_j e^{-i\beta_j z} \right), \quad \frac{d\hat{p}_j}{dz} = i\sqrt{\beta_j} \left(\hat{a}_j e^{i\beta_j z} - \hat{b}_j e^{-i\beta_j z} \right). \quad (2.14)$$

Using these representations, one obtains a system of ordinary differential equations (ODEs) for $\{\hat{a}_j, \hat{b}_j\}$ [10, Section 20.2.4] or [11, Section 3.1]. The coefficients of the system depend on the integrated quantities of the form

$$C_{jl}(z) = \int_{\mathcal{D}} \phi_j(x) \phi_l(x) \nu(x, z) dx. \quad (2.15)$$

This system of ODEs is closed by the boundary conditions at $z = 0$ where the source F is imposed and at $z = \tilde{L}_0 = L_0/\varepsilon^2$ where there is no left-going component.

Forward scattering approximation. Second, we neglect the left-going (backward) propagating mode, assuming that they do not interact with the right-going ones. This is valid in the limit $\varepsilon \rightarrow 0$ when the second-order moments of ν satisfy certain conditions [10, Section 20.2.6] or [11, Section 3.3]. In this case, the rescaled amplitude

$$\hat{a}_j^\varepsilon(z) = \hat{a}_j(\omega, z/\varepsilon^2)$$

of the right-going wave satisfies

$$\frac{d\hat{\mathbf{a}}^\varepsilon}{dz} = \frac{1}{\varepsilon} \mathbf{H}_\omega^{(a)} \left(\frac{z}{\varepsilon^2} \right) \hat{\mathbf{a}}^\varepsilon, \quad (2.16)$$

where $\hat{\mathbf{a}}^\varepsilon$ denotes the $N(\omega)$ -dimensional vector $(\hat{a}_1^\varepsilon, \dots, \hat{a}_{N(\omega)}^\varepsilon)'$ and $\mathbf{H}_\omega^{(a)}$ is a $N(\omega) \times N(\omega)$ complex matrix with components

$$H_{\omega, jl}^{(a)} = \frac{ik^2}{2} \frac{C_{jl}(z)}{\sqrt{\beta_j \beta_l}} e^{i(\beta_l - \beta_j)z}. \quad (2.17)$$

Define the propagator matrix $\mathbf{T}^\varepsilon(\omega, z, z_0)$ to be the fundamental solution of the system (2.16), *i.e.*,

$$\frac{d\mathbf{T}^\varepsilon}{dz}(\omega, z, z_0) = \frac{1}{\varepsilon} \mathbf{H}_\omega^{(a)} \left(\frac{z}{\varepsilon^2} \right) \mathbf{T}^\varepsilon(\omega, z, z_0), \quad (2.18)$$

with $\mathbf{T}^\varepsilon(\omega, z = z_0, z_0) = \mathbf{I}$. Then $\hat{\mathbf{a}}^\varepsilon(\omega, z) = \mathbf{T}^\varepsilon(\omega, z, 0) \hat{\mathbf{a}}^\varepsilon(\omega, 0)$, where the initial amplitude $\hat{\mathbf{a}}^\varepsilon(\omega, 0)$ is determined by the source F . In fact, integrating (2.12) across the plane $z = 0$ and using (2.12, 2.14), we find that

$$\hat{a}_l(\omega, 0) = \frac{1}{2i\sqrt{\beta_l(\omega)}} \hat{f}(\omega) \phi_l(x_s), \quad l = 1, \dots, N(\omega).$$

Consider an array of receivers located in the plane $z = \tilde{L}$ of the random waveguide section, where

$$\tilde{L} = \frac{L}{\varepsilon^2}, \quad (2.19)$$

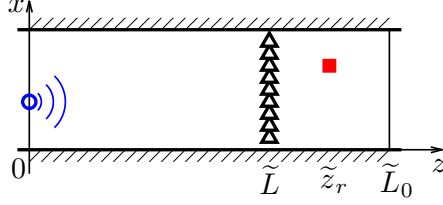


Figure 1: Schematic of the imaging problem. A point source (circle) in the plane $z = 0$ emits a short pulse that propagates through the random waveguide. The target (square) in the plane $z = \tilde{z}_r$ is a reflector. The receiver array (triangles) in the plane $z = \tilde{L}$ records the signals.

and $0 < L < L_0$. Let $T_{jl}^\varepsilon(\omega)$ be the jl -entry of the propagator matrix $\mathbf{T}^\varepsilon(\omega, L, 0)$. It is the rate of conversion of the initial l -mode into the j -mode in the plane $z = \tilde{L} = L/\varepsilon^2$ of the random waveguide section. In particular, we have

$$\hat{a}_j(\omega, \tilde{L}) = \hat{a}_j^\varepsilon(\omega, L) = \sum_{l=1}^{N(\omega)} T_{jl}^\varepsilon(\omega) \hat{a}_l^\varepsilon(\omega, 0) = \sum_{l=1}^{N(\omega)} \frac{1}{2i\sqrt{\beta_l(\omega)}} T_{jl}^\varepsilon(\omega) \hat{f}(\omega) \phi_l(x_s). \quad (2.20)$$

Repeating the argument above, we see that the field beyond \tilde{L} , that is $\hat{\mathbf{a}}(\omega, z) = \{\hat{a}_j(\omega, z)\}_{j=1}^{N(\omega)}$ for $z > \tilde{L} = L/\varepsilon^2$, are related to $\hat{\mathbf{a}}(\omega, \tilde{L}) = \{\hat{a}_j(\omega, \tilde{L})\}_{j=1}^{N(\omega)}$ as follows

$$\hat{a}_j(\omega, z) = \sum_{l=1}^{N(\omega)} T_{jl}^\varepsilon(\omega, \varepsilon^2 z, L) \hat{a}_l^\varepsilon(\omega, L).$$

Since the random waveguide is stationary, $\{T_{jl}^\varepsilon(\omega, z, z_0)\}_{j,l=1}^{N(\omega)}$ has the same distribution as $\{T_{jl}^\varepsilon(\omega, z - z_0, 0)\}_{j,l=1}^{N(\omega)}$. Therefore, we can apply (3.8) and (3.10) in Proposition 3.1 and conclude that $T_{jl}^\varepsilon(\omega, \varepsilon^2 z, L) \approx \delta_{jl}$ in probability provided that $z - \tilde{L} \ll \varepsilon^{-2}$. This is equivalent to say

$$\hat{a}_j(\omega, z) \approx \hat{a}_j(\omega, \tilde{L}), \quad \text{for } 0 \leq z - \tilde{L} \ll \varepsilon^{-2}.$$

Using this approximation and the expressions (2.13) and (2.14), we can write the scalar field at $z > \tilde{L}$ with $z - \tilde{L} \ll \varepsilon^{-2}$ as:

$$\hat{p}(\omega, x, z) = \sum_{j,l=1}^{N(\omega)} \frac{1}{2i\sqrt{\beta_l(\omega)}\sqrt{\beta_j(\omega)}} T_{jl}^\varepsilon(\omega) \hat{f}(\omega) \phi_j(x) \phi_l(x_s) e^{i\beta_j z}. \quad (2.21)$$

2.3 Modeling the point reflector

In the imaging problem to be investigated (see Figure 1), the goal is to locate a point reflector centered at $\mathbf{x}_r = (x_r, \tilde{z}_r)$ from signals recorded at the receiver array in the plane

$z = \tilde{L} = L/\varepsilon^2$. The reflector is supposed to be at a relatively small distance (compared to ε^{-2}), that is to say

$$\tilde{z}_r = \frac{L}{\varepsilon^2} + z_r, \quad 1 \ll z_r \ll \varepsilon^{-2}. \quad (2.22)$$

Note that we also assume that $z_r \gg 1$, i.e. the distance between the reflector and the receiver array is much larger than one (the order of magnitude of the wavelength), to ignore the evanescent modes emitted by the reflector. The reflector can be modeled as a local change in the density and/or the bulk modulus of the medium, so that the sound speed is locally modified as

$$\frac{1}{c^2(x, z)} = \frac{1}{c_0^2}(1 + \varepsilon\nu(x, z)) + \frac{1}{c_r^2}\mathbf{1}_{\Omega_r}(x, z), \quad (2.23)$$

where Ω_r is a small domain around $\mathbf{x}_r := (x_r, \tilde{z}_r)$ which represents the center of the reflector; c_r is a parameter characterizing the contrast of the reflector. With this modification, the right-hand side of (2.5) should have an additional term $-(\omega/c_r)^2\mathbf{1}_{\Omega_r}\hat{p}(\omega, x, z)$. We assume that the diameter of the scattering region Ω_r is small compared to the typical wavelength and that the velocity contrast is such that $\sigma_r := c_r^{-2}|\Omega_r|$ satisfies $\sigma_r \ll 1$. Then we can model the scattering region by a point reflector

$$\frac{1}{c_r^2}\mathbf{1}_{\Omega_r}(x, z) \approx \sigma_r\delta(\mathbf{x} - \mathbf{x}_r).$$

Born approximation. The above setting allows us to solve the scalar field with the presence of the point reflector using the Born approximation for the reflector. Given a fixed frequency ω , we have

$$\hat{p}(\omega, x, z) \approx \hat{p}_p(\omega, x, z) + \hat{p}_s(\omega, x, z). \quad (2.24)$$

Here, \hat{p}_p is the primary field induced by the source F propagating through the random waveguide and computed in the previous section (Eq. (2.21)), and \hat{p}_s is the secondary field, that is the first-order scattered field due to the additional source $-\omega^2\sigma_r\delta(\mathbf{x} - \mathbf{x}_r)\hat{p}_p$ at the reflector:

$$\Delta\hat{p}_s(\omega, x, z) + k^2(\omega)[1 + \varepsilon\nu(x, z)]\hat{p}_s(\omega, x, z) = -\omega^2\sigma_r\delta(\mathbf{x} - \mathbf{x}_r)\hat{p}_p(\omega, x_r, \tilde{z}_r). \quad (2.25)$$

Note that in the Born approximation one replaces the full wave field at the reflector by the primary field in the right-hand side of (2.25).

The primary field is solved exactly as in the previous section. Summarizing the results there, one obtains that for $z \geq \tilde{L}$ and $z - \tilde{L} \ll \varepsilon^{-2}$,

$$\hat{p}_p(\omega, x, z) = \sum_{j,l=1}^{N(\omega)} \frac{\hat{f}(\omega)}{2i\sqrt{\beta_l(\omega)}\sqrt{\beta_j(\omega)}} T_{jl}^\varepsilon(\omega)\phi_j(x)\phi_l(x_s)e^{i\beta_j z}. \quad (2.26)$$

The secondary field satisfies (2.25). Again, we solve this equation using the orthonormal basis $\{\phi_j(x)\}_{j=1,\dots,N(\omega)}$ and we ignore the evanescent modes. Since the reflector is within a distance smaller than ε^{-2} from the receiver array, for $\tilde{L} < z < \tilde{z}_r$, the propagator matrix from \tilde{z}_r to z can be approximated by the identity matrix in probability, and we only need

to decompose the secondary source at the reflector into waveguide modes. Using (2.25), the decomposition (2.14) and the fact that there is no left-going wave from $z > \tilde{z}_r$, we find that

$$\hat{b}_{sj}(\omega, z) = \frac{i\omega^2\sigma_r}{2\sqrt{\beta_j}}\phi_j(x_r)\hat{p}_p(\omega, x_r, \tilde{z}_r). \quad (2.27)$$

We note that there is no right-going secondary wave because we do not consider back-scattering of the left-going secondary wave near the receivers. Finally, recall the expression of the primary field at the reflector (2.26), we obtain for $z \in [\tilde{L}, \tilde{z}_r]$ that

$$\begin{aligned} \hat{p}_s(\omega, x, z) &= \sum_{j=1}^{N(\omega)} \phi_j(x) \frac{1}{\sqrt{\beta_j}} \hat{b}_{sj}(\omega, z) e^{-i\beta_j(z-\tilde{z}_r)} \\ &= \sum_{j,l,m=1}^{N(\omega)} \frac{\omega^2\sigma_r\hat{f}(\omega)}{4\beta_j\sqrt{\beta_m}\sqrt{\beta_l}} T_{lm}^\varepsilon(\omega) \phi_j(x) \phi_j(x_r) \phi_l(x_r) \phi_m(x_s) e^{-i\beta_j(z-\tilde{z}_r)} e^{i\beta_l\tilde{z}_r}. \end{aligned} \quad (2.28)$$

3 Migration-Based Imaging Functional

In this section, we introduce the classical imaging functional to localize the point reflector using the scalar (pressure) field recorded at the receiver array at $z = \tilde{L}$. This imaging functional is based on the migration of the array data to a search point (x^S, \tilde{z}^S) . Our goal is to show that classical Kirchhoff migration functional does not give a good image when the medium between the source at $z = 0$ and the receiver array at $z = \tilde{L}$ is scattering.

The data of scalar (pressure) field recorded by the receivers are

$$\{p(t, x, \tilde{L}) \mid t \in \mathbb{R}, x \in \mathcal{D}\}.$$

Note that we consider in this section the full aperture case: the receivers span the whole cross section of the waveguide and they record data at all time. We consider the frequency- and mode-dependent data

$$\hat{p}_j(\omega, z = \tilde{L}) = \int \int p(t, x, z = \tilde{L}) \phi_j(x) dx e^{i\omega t} dt.$$

According to the analysis carried out Section 2.3, it can be decomposed as

$$\hat{p}_j(\omega, z = \tilde{L}) = \hat{p}_{pj}(\omega, z = \tilde{L}) + \hat{p}_{sj}(\omega, z = \tilde{L}).$$

From (2.26) and (2.28) the primary and secondary contributions are

$$\hat{p}_{pj}(\omega, z = \tilde{L}) = \frac{\hat{f}(\omega)}{2i\sqrt{\beta_j(\omega)}} e^{i\beta_j\frac{\tilde{L}}{\varepsilon^2}} \sum_{l=1}^N \frac{T_{jl}^\varepsilon(\omega)}{\sqrt{\beta_l}} \phi_l(x_s), \quad (3.1)$$

$$\hat{p}_{sj}(\omega, z = \tilde{L}) = \frac{1}{\beta_j(\omega)} \phi_j(x_r) e^{i\beta_j\tilde{z}_r} q(\omega, x_r, \tilde{z}_r), \quad (3.2)$$

with

$$q(\omega, x_r, \tilde{z}_r) = \sum_{l,m=1}^N \frac{\omega^2\hat{f}(\omega)\sigma_r}{4\sqrt{\beta_m(\omega)}\sqrt{\beta_l(\omega)}} T_{lm}^\varepsilon(\omega) \phi_l(x_r) \phi_m(x_s) e^{i\beta_l(\omega)\tilde{z}_r},$$

which can be interpreted as an illumination of the reflector. The secondary contribution \hat{p}_{sj} contains the information about the reflector, and its form (3.2) motivates the definition of the Kirchhoff migration imaging functional:

$$\mathcal{I}_{\text{KM}}(x^{\text{S}}, z^{\text{S}}) = \frac{1}{2\pi} \int \frac{1}{N(\omega)} \sum_{j=1}^{N(\omega)} \beta_j(\omega) \phi_j(x^{\text{S}}) e^{-i\beta_j(\omega)z^{\text{S}}} \hat{p}_j(\omega, z = \tilde{L}) d\omega, \quad (3.3)$$

where the search point is $(x^{\text{S}}, \tilde{z}^{\text{S}})$ with $\tilde{z}^{\text{S}} = \tilde{L} + z^{\text{S}}$.

A simple case is when the source term is time-harmonic, *i.e.* $F(t, \mathbf{x}) = \delta(\mathbf{x} - \mathbf{x}_{\text{source}})f(t)$ with $f(t) = e^{-i\omega_0 t}$ and

$$\hat{f}(\omega) = 2\pi\delta(\omega - \omega_0).$$

Then the data set is reduced to $\{\hat{p}_j(\omega_0, z = \tilde{L}), j = 1, \dots, N(\omega_0)\}$ and the Kirchhoff migration functional has the form

$$\mathcal{I}_{\text{KM}}(x^{\text{S}}, z^{\text{S}}) = \frac{1}{N(\omega_0)} \sum_{j=1}^{N(\omega_0)} \beta_j(\omega_0) \phi_j(x^{\text{S}}) e^{-i\beta_j(\omega_0)z^{\text{S}}} \hat{p}_j(\omega_0, z = \tilde{L}). \quad (3.4)$$

We need to compute the mean of the imaging functional in order to characterize its resolution properties and its variance in order to characterize its stability properties. These statistical moments depend on the moments of the propagator matrix which were studied in [10, Propositions 20.6 and 20.8] or [11, Propositions 6.1 and 6.3].

Proposition 3.1. *The first-order moments of the transmission coefficients have limits as $\varepsilon \rightarrow 0$, which are given by*

$$\mathbb{E}[T_{jl}^\varepsilon(\omega)] \xrightarrow{\varepsilon \rightarrow 0} 0, \quad \text{if } j \neq l, \quad (3.5)$$

$$\mathbb{E}[T_{jj}^\varepsilon(\omega)] \xrightarrow{\varepsilon \rightarrow 0} e^{-D_j(\omega)L}, \quad \text{otherwise.} \quad (3.6)$$

The second-order moments of the transmission coefficients have limits as $\varepsilon \rightarrow 0$, which are given by

$$\mathbb{E}[T_{jj}^\varepsilon(\omega)\overline{T_{ll}^\varepsilon(\omega)}] \xrightarrow{\varepsilon \rightarrow 0} e^{-Q_{jl}(\omega)L}, \quad \text{if } j \neq l, \quad (3.7)$$

$$\mathbb{E}[T_{jl}^\varepsilon(\omega)\overline{T_{jl}^\varepsilon(\omega)}] \xrightarrow{\varepsilon \rightarrow 0} \mathcal{T}_j^{(l)}(\omega, L), \quad (3.8)$$

$$\mathbb{E}[T_{jl}^\varepsilon(\omega)\overline{T_{mn}^\varepsilon(\omega)}] \xrightarrow{\varepsilon \rightarrow 0} 0, \quad \text{otherwise.} \quad (3.9)$$

The functions $\mathcal{T}_j^{(l)}(\omega, z)$ are the solutions of the system of linear equations

$$\frac{d\mathcal{T}_j^{(l)}}{dz} = \sum_{n \neq j} \Gamma_{jn}^{(c)}(\omega) \left(\mathcal{T}_n^{(l)} - \mathcal{T}_j^{(l)} \right), \quad \mathcal{T}_j^{(l)}(\omega, z = 0) = \delta_{jl}. \quad (3.10)$$

The positive coefficients D_j and Q_{jl} and the matrix $\Gamma_{jn}^{(c)}$ depend on the correlation function of the random process ν . Furthermore, we have

$$\sup_{j,l} |\mathbb{E}[T_{jl}^\varepsilon(\omega)]| \leq C e^{-L/L_{\text{equip}}}, \quad \sup_{j,l} \left| \mathcal{T}_j^{(l)}(\omega, L) - \frac{1}{N} \right| \leq C e^{-L/L_{\text{equip}}}, \quad (3.11)$$

where L_{equip} is the equipartition distance for the mean mode powers introduced at the end of Section 20.3.3 in [10] (or at the end of Section 4.2 in [11]).

The results on the first-order moments describe how the wave loses its coherence as it propagates in the random waveguide. The results on the second-order moments describe how the wave energy becomes equipartitioned on the waveguide modes.

When L is larger than the energy equipartition length L_{equip} , then the first-order moments of the transmission coefficients are vanishing. Based on this observation, we have

$$\mathbb{E}[\mathcal{I}_{\text{KM}}(x^{\text{S}}, z^{\text{S}})] \approx 0. \quad (3.12)$$

It turns out that the fluctuations of the imaging functional are much larger than its mean. This can be seen by studying the standard deviation of the imaging functional. When L is larger than the energy equipartition length L_{equip} , then the second-order moments of the transmission coefficients are vanishing except $\mathbb{E}[|T_{jl}^\varepsilon|^2]$ which converge to $1/N$. Based on this observation, the second-order moment of the imaging functional for a time-harmonic source is:

$$\begin{aligned} \mathbb{E}[|\mathcal{I}_{\text{KM}}(x^{\text{S}}, z^{\text{S}})|^2] &= \frac{|\hat{f}(\omega_0)|^2 \Phi_{-1}(x_s)}{N} \left[\frac{1}{4} \Phi_1(x^{\text{S}}) + \left(\frac{\omega^2 \sigma_r N}{4} \right)^2 \Phi_{-1}(x_r) |\Psi(x^{\text{S}}, z^{\text{S}}; x_r, z_r)|^2 \right. \\ &\quad \left. + \left(\frac{\omega^2 \sigma_r N}{4} \right) \Im m(\Psi(x^{\text{S}}, -z^{\text{S}}; x_r, -z_r) \Psi(x^{\text{S}}, z^{\text{S}}; x_r, -z_r)) \right], \end{aligned} \quad (3.13)$$

where, for any integer j , we have defined

$$\Phi_j(x) = \frac{1}{N} \sum_{n=1}^N \beta_n^j \phi_n^2(x), \quad (3.14)$$

$$\Psi(x^{\text{S}}, z^{\text{S}}; x_r, z_r) = \frac{1}{N} \sum_{n=1}^N \phi_n(x_r) \phi_n(x^{\text{S}}) e^{i\beta_n(z_r - z^{\text{S}})}. \quad (3.15)$$

The first term in the right-hand side of (3.13) is the contribution of the primary field. The second term is the contribution of the secondary field. The third term is a crossed contribution.

These results show that, when the waveguide is randomly perturbed and long enough (longer than the equipartition distance), then the illumination of the reflector becomes incoherent and Kirchhoff migration, which is based on coherent effects, gives a completely unstable and noisy image.

The analysis is complete in the time-harmonic case. The analysis of the broadband case (when the support of the source spectrum is not reduced to a single carrier frequency) goes along the same line although it is necessary to use the asymptotic expressions of the two-frequency second-order moments of the transmission coefficients (see [10, Proposition 20.7] or [11, Proposition 6.3]): due to the loss of coherence, the mean of the imaging functional is zero while its variance is not.

4 Correlation-Based Imaging Functionals

In this section, we introduce a new imaging functional to localize the point reflector using the scalar field recorded at the receiver array at $z = \tilde{L}$. This functional is based on the correlation functions of the recorded signals, which we stress in the first subsection.

4.1 Correlation of the scalar field

Let \mathcal{A} denote the positions of the receivers in the plane $z = \tilde{L}$. The data of scalar (pressure) field recorded by the receivers are $\{p^\varepsilon(t, x, \tilde{L}) \mid t \in \mathbb{R}, x \in \mathcal{A}\}$. For simplicity, we have assumed that the receivers record data at all time. From these data one can form the cross correlation of the recorded field:

$$\mathcal{C}(\tau, x_1, x_2) = \int_{\mathbb{R}} \overline{p}(t, x_1, \tilde{L}) p(t + \tau, x_2, \tilde{L}) dt, \quad x_1, x_2 \in \mathcal{A}. \quad (4.1)$$

In Fourier domain, it has the form:

$$\mathcal{C}(\tau, x_1, x_2) = \frac{1}{2\pi} \int_{\mathbb{R}} \overline{\hat{p}}(\omega, x_1, \tilde{L}) \hat{p}(\omega, x_2, \tilde{L}) e^{-i\omega\tau} d\omega, \quad x_1, x_2 \in \mathcal{A}. \quad (4.2)$$

Using the decomposition $\hat{p} = \hat{p}_p + \hat{p}_s$ in (2.24), we can decompose the above cross correlation function into four parts. Let \mathcal{C}_{pp} denote the cross correlation between the primary fields at the two receivers. Thanks to the formula (2.26), it admits the expression

$$\begin{aligned} \mathcal{C}_{pp}(\tau, x_1, x_2) &= \frac{1}{8\pi} \int \sum_{j,l,m,n=1}^{N(\omega)} \frac{1}{\sqrt{\beta_l \beta_n \beta_j \beta_m}(\omega)} \overline{T_{jl}^\varepsilon}(\omega) T_{mn}^\varepsilon(\omega) |\hat{f}(\omega)|^2 \phi_j(x_1) \phi_m(x_2) \\ &\quad \phi_l(x_s) \phi_n(x_s) e^{i(\beta_m - \beta_j)\tilde{L}} e^{-i\omega\tau} d\omega. \end{aligned} \quad (4.3)$$

Let \mathcal{C}_{ps} denote the cross correlation between the primary field at the first receiver with the secondary field at the second receiver. Recall that the secondary field contains information about the waves emitted from the reflector at $\mathbf{x}_r = (x_r, \tilde{z}_r)$, with $\tilde{z}_r = \tilde{L} + z_r$. Due to (2.26) and (2.28), it admits the expression

$$\begin{aligned} \mathcal{C}_{ps}(\tau, x_1, x_2) &= \int \sum_{q,j,l,m,n=1}^{N(\omega)} \frac{i\omega^2 \sigma_r}{16\pi \beta_q \sqrt{\beta_l \beta_n \beta_j \beta_m}(\omega)} \overline{T_{jl}^\varepsilon}(\omega) T_{mn}^\varepsilon(\omega) |\hat{f}(\omega)|^2 \phi_j(x_1) \phi_q(x_2) \\ &\quad \phi_l(x_s) \phi_n(x_s) \phi_q(x_r) \phi_m(x_r) e^{i(\beta_m - \beta_j)\tilde{L}} e^{i(\beta_q + \beta_m)z_r} e^{-i\omega\tau} d\omega. \end{aligned} \quad (4.4)$$

Similarly, let \mathcal{C}_{sp} denote the cross correlation between the secondary field at the first receiver with the primary field at the second receiver. One verifies that

$$\begin{aligned} \mathcal{C}_{sp}(\tau, x_1, x_2) &= \int \sum_{q,j,l,m,n=1}^{N(\omega)} \frac{-i\omega^2 \sigma_r}{16\pi \beta_q \sqrt{\beta_l \beta_n \beta_j \beta_m}(\omega)} \overline{T_{jl}^\varepsilon}(\omega) T_{mn}^\varepsilon(\omega) |\hat{f}(\omega)|^2 \phi_q(x_1) \phi_m(x_2) \\ &\quad \phi_l(x_s) \phi_n(x_s) \phi_q(x_r) \phi_j(x_r) e^{i(\beta_m - \beta_j)\tilde{L}} e^{-i(\beta_q + \beta_j)z_r} e^{-i\omega\tau} d\omega. \end{aligned} \quad (4.5)$$

Finally, the cross correlation between the secondary fields at the two receivers is much smaller than those above and its contribution is ignored. We neglected also the contributions from the error terms of the decomposition (2.24). These are justified because $\sigma_r \ll 1$ consistently with the Born approximation.

Recall that the source in the acoustic model is due to the force $F(t, \mathbf{x}) = f(t)\delta(\mathbf{x} - \mathbf{x}_{\text{source}})$ where $\mathbf{x}_{\text{source}} = (x_s, 0)$ indicates the location of the source. In the rest of the paper, we will consider two special cases as follows.

4.1.1 Cross correlation for broadband pulse

We first consider the case where the source is given by $F(t, \mathbf{x}) = f(t)\delta(\mathbf{x} - \mathbf{x}_{\text{source}})$ with

$$f(t) = f_0(\varepsilon^\alpha t)e^{-i\omega_0 t}. \quad (4.6)$$

Here, ω_0 is the carrier frequency. In the Fourier domain, we have

$$\hat{f}(\omega) = \frac{1}{\varepsilon^\alpha} \hat{f}_0\left(\frac{\omega - \omega_0}{\varepsilon^\alpha}\right).$$

Here, \hat{f}_0 is assumed to be a function with compact support or fast decay.

When $\alpha \geq 2$ the bandwidth has no effect and the situation is equivalent to the time-harmonic case that we address in the next section.

When $\alpha = (0, 2)$, the pulse is said to be broadband and the bandwidth plays a role in the propagation in the waveguide for a propagation distance of the order of $\tilde{L} = L/\varepsilon^2$. Although the analysis can be carried out in general, we restrict ourselves to the case $\alpha \in (1, 2)$ because when $\alpha \leq 1$, the number of propagating modes $N(\omega)$ varies with ω over the bandwidth and the analysis is a little bit more delicate. Nevertheless, the overall picture does not change in the latter case.

Henceforth, α is a fixed number in the interval $(1, 2)$. Let $\omega = \omega_0 + \varepsilon^\alpha h$. Then

$$\hat{f}(\omega) = \frac{1}{\varepsilon^\alpha} \hat{f}_0(h), \quad T_{jl}^\varepsilon(\omega) = T_{jl}^\varepsilon(\omega_0 + \varepsilon^\alpha h),$$

in terms of the new variable h . Further, we have the following Taylor expansions

$$\beta_j(\omega) = \beta_j + \varepsilon^\alpha \beta'_j h + o(\varepsilon^\alpha), \quad \frac{1}{\sqrt{\beta_j \beta_m \beta_l \beta_n}(\omega)} = \frac{1}{\sqrt{\beta_j \beta_m \beta_l \beta_n}} + O(\varepsilon^\alpha).$$

Here, β'_j is the derivative of β_j at the carrier frequency ω_0 ; further, the reduced wavenumber β_j is also evaluated at ω_0 . Using these formulas, the cross correlation functions become

$$\mathcal{C}_{\text{pp}}(\tau, x_1, x_2) \approx \frac{1}{8\pi\varepsilon^\alpha} \int \sum_{j,l,m,n=1}^N \frac{|\hat{f}_0(h)|^2}{\sqrt{\beta_j \beta_m \beta_l \beta_n}} \overline{T_{jl}^\varepsilon}(\omega_0 + \varepsilon^\alpha h) T_{mn}^\varepsilon(\omega_0 + \varepsilon^\alpha h) \phi_j(x_1) \phi_m(x_2)$$

$$\phi_l(x_s) \phi_n(x_s) e^{i[\beta_m(\omega_0 + \varepsilon^\alpha h) - \beta_j(\omega_0 + \varepsilon^\alpha h)]\tilde{L}} e^{-i(\omega_0 + \varepsilon^\alpha h)\tau} dh,$$

$$\mathcal{C}_{\text{ps}} \approx \int \sum_{q,j,l,m,n=1}^N \frac{i\omega_0^2 \sigma_r}{16\pi\beta_q \varepsilon^\alpha} \frac{|\hat{f}_0(h)|^2}{\sqrt{\beta_j \beta_m \beta_l \beta_n}} \overline{T_{jl}^\varepsilon}(\omega_0 + \varepsilon^\alpha h) T_{mn}^\varepsilon(\omega_0 + \varepsilon^\alpha h) \phi_j(x_1) \phi_q(x_2) \phi_l(x_s)$$

$$\phi_n(x_s) \phi_q(x_r) \phi_m(x_r) e^{i[\beta_m(\omega_0 + \varepsilon^\alpha h) - \beta_j(\omega_0 + \varepsilon^\alpha h)]\tilde{L}} e^{i(\beta_q + \beta_m)z_r} e^{i(\beta'_q + \beta'_m)\varepsilon^\alpha h z_r} e^{-i(\omega_0 + \varepsilon^\alpha h)\tau} dh,$$

$$\begin{aligned} \mathcal{C}_{\text{sp}} \approx & \int \sum_{q,j,l,m,n=1}^N \frac{-i\omega_0^2 \sigma_r}{16\pi\beta_q \varepsilon^\alpha} \frac{|\hat{f}_0(h)|^2}{\sqrt{\beta_j \beta_m \beta_l \beta_n}} \overline{T_{jl}^\varepsilon}(\omega_0 + \varepsilon^\alpha h) T_{mn}^\varepsilon(\omega_0 + \varepsilon^\alpha h) \phi_q(x_1) \phi_m(x_2) \phi_l(x_s) \\ & \phi_n(x_s) \phi_q(x_r) \phi_j(x_r) e^{i[\beta_m(\omega_0 + \varepsilon^\alpha h) - \beta_j(\omega_0 + \varepsilon^\alpha h)]\tilde{L}} e^{-i(\beta_q + \beta_j)z_r} e^{-i(\beta'_q + \beta'_j)\varepsilon^\alpha h z_r} e^{-i(\omega_0 + \varepsilon^\alpha h)\tau} dh. \end{aligned}$$

4.1.2 Cross correlation with time-harmonic source

A simple case is when the source term is time-harmonic, *i.e.* $F(t, \mathbf{x}) = \delta(\mathbf{x} - \mathbf{x}_{\text{source}})f(t)$ with $f(t) = e^{-i\omega_0 t}$ and

$$\hat{f}(\omega) = 2\pi\delta(\omega - \omega_0).$$

In this case, the wave field has the form $p(t, x, z) = \hat{p}(x, z; \omega_0)e^{-i\omega_0 t}$. The definition of the correlation function should be modified to

$$\mathcal{C}(\tau, x_1, x_2) := \frac{1}{T} \int_0^T \overline{p}(t, x_1, \tilde{L}) p(t + \tau, x_2, \tilde{L}) dt = e^{-i\omega_0 \tau} \overline{\hat{p}}(x_1, \tilde{L}; \omega_0) \hat{p}(x_2, \tilde{L}; \omega_0). \quad (4.7)$$

The second equality holds because the integrand above is in fact independent of t . Using the decomposition (2.24) and the expressions (2.26) and (2.28), we obtain the following expressions for the cross correlations:

$$\begin{aligned} \mathcal{C}_{\text{pp}}(\tau, x_1, x_2) &= \frac{1}{4} \sum_{j,l,m,n=1}^{N(\omega_0)} \frac{1}{\sqrt{\beta_j \beta_m \beta_l \beta_n}} \overline{T_{jl}^\varepsilon}(\omega_0) T_{mn}^\varepsilon(\omega_0) \phi_j(x_1) \phi_m(x_2) \\ & \quad \phi_l(x_s) \phi_n(x_s) e^{i(\beta_m - \beta_j)\tilde{L}} e^{-i\omega_0 \tau}, \\ \mathcal{C}_{\text{ps}}(\tau, x_1, x_2) &= \sum_{q,j,l,m,n=1}^{N(\omega_0)} \frac{i\omega_0^2 \sigma_r}{8\beta_q} \frac{1}{\sqrt{\beta_j \beta_m \beta_l \beta_n}} \overline{T_{jl}^\varepsilon}(\omega_0) T_{mn}^\varepsilon(\omega_0) \phi_j(x_1) \phi_q(x_2) \\ & \quad \phi_l(x_s) \phi_n(x_s) \phi_q(x_r) \phi_m(x_r) e^{i(\beta_m - \beta_j)\tilde{L}} e^{i(\beta_q + \beta_m)z_r} e^{-i\omega_0 \tau}, \\ \mathcal{C}_{\text{sp}}(\tau, x_1, x_2) &= \sum_{q,j,l,m,n=1}^{N(\omega_0)} \frac{-i\omega_0^2 \sigma_r}{8\beta_q} \frac{1}{\sqrt{\beta_j \beta_m \beta_l \beta_n}} \overline{T_{jl}^\varepsilon}(\omega_0) T_{mn}^\varepsilon(\omega_0) \phi_q(x_1) \phi_m(x_2) \\ & \quad \phi_l(x_s) \phi_n(x_s) \phi_q(x_r) \phi_j(x_r) e^{i(\beta_m - \beta_j)\tilde{L}} e^{-i(\beta_q + \beta_j)z_r} e^{-i\omega_0 \tau}. \end{aligned}$$

4.2 Imaging functionals using cross correlations

We are now ready to present the imaging functionals, which consist in migrating the cross correlations of the recorded signals. The imaging functionals are designed according to the settings of receiver arrays. We consider two cases.

Full aperture receiver array. The ideal case is when the receiver array spans the whole cross section, *i.e.*, $\mathcal{A} = \mathcal{D}$. Then given the data, for any pair of modes ϕ_j and ϕ_l , we define

$$\mathcal{C}^{jl}(\tau) := \int_{\mathcal{A}} \int_{\mathcal{A}} \mathcal{C}(\tau, x_1, x_2) \phi_j(x_1) \phi_l(x_2) dx_1 dx_2. \quad (4.8)$$

Due to the orthogonality of $\{\phi_j\}_{j=1,\dots,N}$, the function \mathcal{C}^{jl} is the jl mode of the cross correlation function \mathcal{C} .

A search point for the reflector will be denoted as (x^S, \tilde{z}^S) where x^S is its transversal coordinate and $\tilde{z}^S = \tilde{L} + z^S$ is its axial coordinate. Equivalently, z^S is the axial coordinate starting from the receiver array. We define the imaging functional \mathcal{I}_{FA} as

$$\mathcal{I}_{\text{FA}}(x^S, z^S) = \mathcal{I}_{\text{FA}+}(x^S, z^S) + \mathcal{I}_{\text{FA}-}(x^S, z^S), \quad (4.9)$$

$$\mathcal{I}_{\text{FA}\pm}(x^S, z^S) = \mp \frac{i}{N(\omega_0)^2} \sum_{j,l=1}^{N(\omega_0)} \beta_j \beta_l(\omega_0) \phi_j(x^S) \phi_l(x^S) \mathcal{C}^{jl} \left(\pm \frac{z^S}{\omega_0} (\beta_j + \beta_l) \right). \quad (4.10)$$

The choice of multiplication by $\beta_j \beta_l$ is suggested from our analysis of the correlation functions in the next section.

Limited aperture receiver array. A realistic situation is when the receiver array only covers part of the transversal section, *i.e.*, $\mathcal{A} = [a_1, a_2]$ for $0 < a_1 < a_2 < a$. Consequently, the exact jl component of the cross correlation cannot be extracted. In this case, we design the following imaging functional \mathcal{I}_{LA} as

$$\mathcal{I}_{\text{LA}}(x^S, z^S) = \mathcal{I}_{\text{LA}+}(x^S, z^S) + \mathcal{I}_{\text{LA}-}(x^S, z^S), \quad (4.11)$$

$$\begin{aligned} \mathcal{I}_{\text{LA}\pm}(x^S, z^S) &= \mp \frac{i}{N(\omega_0)^2} \int_{\mathcal{A}^2} \sum_{j,q=1}^{N(\omega_0)} \phi_q(x_1) \phi_q(x^S) \phi_j(x_2) \phi_j(x^S) \\ &\quad \times (\Delta_{x_1} + k(\omega_0)^2) (\Delta_{x_2} + k(\omega_0)^2) \mathcal{C} \left(\pm \frac{z^S}{\omega_0} (\beta_q + \beta_j), x_1, x_2 \right) dx_1 dx_2. \end{aligned} \quad (4.12)$$

Again, these definitions of imaging functionals are based on the analysis of the correlation functions in the next section. We remark also that it is possible to show that when $\mathcal{A} = \mathcal{D}$, the second functional \mathcal{I}_{LA} is very close to \mathcal{I}_{FA} and we have in fact:

$$\mathcal{I}_{\text{LA}\pm}(x^S, z^S) |_{\mathcal{A}=\mathcal{D}} = \mp \frac{i}{N(\omega_0)^2} \sum_{j,l=1}^{N(\omega_0)} \beta_j^2 \beta_l^2(\omega_0) \phi_j(x^S) \phi_l(x^S) \mathcal{C}^{jl} \left(\pm \frac{z^S}{\omega_0} (\beta_j + \beta_l) \right).$$

5 Resolution Analysis of the Imaging Functionals

In this section, we analyze the imaging functionals proposed above to search the reflectors in the waveguide. Due to the random perturbations of the long section $z \in [0, \tilde{L}]$ of the waveguide, the values of the imaging functionals, which depend on the waveguide parameters through the data, are random. Hence, we analyze the mean of the imaging functional and show that it achieves its maximum at the reflector location. We also analyze how this mean decays from its maximum; this information provides the resolution of the proposed imaging functionals.

We emphasize that the above observation on the mean of the imaging functional itself is not enough to claim that the functionals are effective, because it is not certain, *a priori*, that the one realization in practice is well reflected by the mean. Statistical stability (*i.e.*, the analysis of the fluctuations of the imaging functionals) is needed to secure this claim. This will be investigated in the Section 6.

5.1 The case of full aperture receiver array with time-harmonic sources

We first consider the ideal case where the receiver array \mathcal{A} spans the whole cross section, so the imaging functional \mathcal{I}_{FA} is chosen. The key tool for analysis of the mean of \mathcal{I}_{FA} is Proposition 3.1.

As shown by Proposition 3.1, when L is larger than the energy equipartition length L_{equip} , the main contribution from terms of $\mathbb{E}\{T_{jl}^\varepsilon T_{mn}^\varepsilon\}$ comes from when $j = m$ and $l = n$. Following this observation, we have the following limits for the cross correlations.

$$\mathbb{E}\{\mathcal{C}_{\text{pp}}(\tau, x_1, x_2)\} \rightarrow \frac{\Phi_{-1}(x_s)}{4} \sum_{j=1}^N \frac{1}{\beta_j} \phi_j(x_1) \phi_j(x_2) e^{-i\omega_0 \tau},$$

where Φ_{-1} is defined by (3.14) and we have also used the fact that $\mathcal{T}_j^{(l)}$ converges to $1/N$ in the regime $L \gg L_{\text{equip}}$.

Following the same lines, we have

$$\mathbb{E}\{\mathcal{C}_{\text{ps}}(\tau, x_1, x_2)\} \rightarrow \frac{i\omega_0^2 \sigma_r \Phi_{-1}(x_s)}{8} \sum_{q,j=1}^{N(\omega_0)} \frac{1}{\beta_j \beta_q} \phi_j(x_1) \phi_j(x_r) \phi_q(x_r) \phi_q(x_2) e^{i(\beta_j + \beta_q) z_r} e^{-i\omega_0 \tau}, \quad (5.1)$$

and

$$\mathbb{E}\{\mathcal{C}_{\text{sp}}(\tau, x_1, x_2)\} \rightarrow \frac{-i\omega_0^2 \sigma_r \Phi_{-1}(x_s)}{8} \sum_{q,j=1}^{N(\omega_0)} \frac{1}{\beta_j \beta_q} \phi_q(x_1) \phi_q(x_r) \phi_j(x_r) \phi_j(x_2) e^{-i(\beta_q + \beta_j) z_r} e^{-i\omega_0 \tau}. \quad (5.2)$$

In fact, the migration imaging functional \mathcal{I}_{FA} is designed from the above characterization of the cross correlation function. From the calculations before, we find

$$\mathbb{E}\{\mathcal{C}_{\text{pp}}^{jl}(\tau)\} \rightarrow \frac{\Phi_{-1}(x_s)}{4\beta_j} \delta_{jl} e^{-i\omega_0 \tau},$$

where δ_{jl} is the Kronecker symbol. We also find

$$\begin{aligned} \mathbb{E}\{\mathcal{C}_{\text{ps}}^{jl}(\tau)\} &\rightarrow \frac{i\omega_0^2 \sigma_r \Phi_{-1}(x_s)}{8} \frac{1}{\beta_j \beta_l} \phi_j(x_r) \phi_l(x_r) e^{i(\beta_j + \beta_l) z_r} e^{-i\omega_0 \tau}. \\ \mathbb{E}\{\mathcal{C}_{\text{sp}}^{jl}(\tau)\} &\rightarrow \frac{-i\omega_0^2 \sigma_r \Phi_{-1}(x_s)}{8} \frac{1}{\beta_j \beta_l} \phi_j(x_r) \phi_l(x_r) e^{-i(\beta_j + \beta_l) z_r} e^{-i\omega_0 \tau}. \end{aligned}$$

Therefore, for a search point (x^S, \tilde{z}^S) , with $\tilde{z}^S = \tilde{L} + z^S$, we have the following. From now on, $\lambda = 2\pi/k(\omega_0)$ denotes the carrier wavelength.

Proposition 5.1. *If $a \gg \lambda$, $z^S, z_r \gg \lambda$, and $x^S, x_r \in (0, a)$, then*

$$\mathbb{E}[\mathcal{I}_{\text{FA}}(x^S, z^S)] \simeq \frac{\pi\omega_0^2 \sigma_r}{32a^3} \Re e \left\{ \left[\int_{-\frac{\pi}{2}}^{\frac{\pi}{2}} \cos \theta e^{i(\tilde{\eta} \cos \theta + \tilde{\xi} \sin \theta)} d\theta \right]^2 \right\}, \quad (5.3)$$

where we have introduced the normalized cross range offset $\tilde{\xi} = 2\pi(x_r - x^S)/\lambda$, and the normalized range offset $\tilde{\eta} = 2\pi(z_r - z^S)/\lambda$.

Therefore, the imaging functional \mathcal{I}_{FA} works well to detect the point reflector (x_r, \tilde{z}_r) . In particular we can see that both the range and cross-range resolutions are of the order of the wavelength λ .

Proof. Note that $a \gg \lambda$ means that $N \gg 1$. Calculations show that

$$\begin{aligned} \mathbb{E}[\mathcal{I}_{\text{FA}+}(x^{\text{S}}, z^{\text{S}})] &\rightarrow \frac{-i\Phi_{-1}(x_{\text{s}})}{4N} \left[\frac{1}{N} \sum_{j=1}^N \beta_j \phi_j^2(x^{\text{S}}) e^{-i2\beta_j z^{\text{S}}} \right] \\ &\quad + \frac{\omega_0^2 \sigma_{\text{r}} \Phi_{-1}(x_{\text{s}})}{8} \Psi(x^{\text{S}}, z^{\text{S}}; x_{\text{r}}, z_{\text{r}})^2 - \frac{\omega_0^2 \sigma_{\text{r}} \Phi_{-1}(x_{\text{s}})}{8} \Psi(x^{\text{S}}, z^{\text{S}}; x_{\text{r}}, -z_{\text{r}})^2, \end{aligned} \quad (5.4)$$

where Ψ and Φ_j are defined by (3.15) and (3.14). The first term does not contain information about the reflector and can be viewed as background field. In fact, its contribution is negligible because the fast oscillations in the complex exponential ($z_{\text{r}}, z^{\text{S}} \gg \lambda$) average out and there is an overall factor $1/N$. For the second term, we can use an integral approximation for the sum in the continuum limit ($N \gg 1$). That is,

$$\begin{aligned} \Psi(x^{\text{S}}, z^{\text{S}}; x_{\text{r}}, z_{\text{r}}) &= \frac{1}{N} \sum_{j=1}^N \frac{2}{a} \sin\left(\frac{2\pi x^{\text{S}}}{\lambda} \frac{j}{N}\right) \sin\left(\frac{2\pi x_{\text{r}}}{\lambda} \frac{j}{N}\right) e^{i2\pi \sqrt{1 - (\frac{j}{N})^2} \frac{(z_{\text{r}} - z^{\text{S}})}{\lambda}} \\ &= \frac{1}{aN} \sum_{j=1}^N \left(\cos\left(\frac{2\pi(x_{\text{r}} - x^{\text{S}})}{\lambda} \frac{j}{N}\right) - \cos\left(\frac{2\pi(x_{\text{r}} + x^{\text{S}})}{\lambda} \frac{j}{N}\right) \right) e^{i2\pi \sqrt{1 - (\frac{j}{N})^2} \frac{z_{\text{r}} - z^{\text{S}}}{\lambda}} \\ &\approx \frac{1}{a} \int_0^1 \left(\cos\left(\frac{2\pi(x_{\text{r}} - x^{\text{S}})}{\lambda} y\right) - \cos\left(\frac{2\pi(x_{\text{r}} + x^{\text{S}})}{\lambda} y\right) \right) e^{i2\pi \sqrt{1 - y^2} \frac{z_{\text{r}} - z^{\text{S}}}{\lambda}} dy. \end{aligned}$$

Since the phase becomes zero when $z^{\text{S}} = z_{\text{r}}$, this function peaks at $z^{\text{S}} = z_{\text{r}}$ and $x^{\text{S}} = x_{\text{r}}$. The integral considered above can be written as, with the second term neglected,

$$\begin{aligned} \frac{1}{2a} \int_0^1 e^{i(\tilde{\eta}\sqrt{1-y^2} + \tilde{\xi}y)} + e^{i(\tilde{\eta}\sqrt{1-y^2} - \tilde{\xi}y)} dy &= \frac{1}{2a} \int_{-1}^1 e^{i(\tilde{\eta}\sqrt{1-y^2} + \tilde{\xi}y)} dy \\ &= \frac{1}{2a} \int_{-\frac{\pi}{2}}^{\frac{\pi}{2}} \cos \theta e^{i(\tilde{\eta} \cos \theta + \tilde{\xi} \sin \theta)} d\theta. \end{aligned}$$

Similarly, the sum in the third term can be approximated by

$$\Psi(x^{\text{S}}, z^{\text{S}}; x_{\text{r}}, -z_{\text{r}}) \approx \frac{1}{a} \int_0^1 \left(\cos\left(\frac{2\pi(x_{\text{r}} - x^{\text{S}})}{\lambda} y\right) - \cos\left(\frac{2\pi(x_{\text{r}} + x^{\text{S}})}{\lambda} y\right) \right) e^{-i2\pi \sqrt{1 - y^2} \frac{z_{\text{r}} + z^{\text{S}}}{\lambda}} dy.$$

Note that this function does not have a peak comparable with the previous function. In fact, stationary phase calculation shows that it is of order $O(1/(a\sqrt{k(z_{\text{r}} + z^{\text{S}})}))$ where $k = 2\pi/\lambda$.

The evaluation of $\mathbb{E}[\mathcal{I}_{\text{FA}-}]$ follows the same lines:

$$\begin{aligned} \mathbb{E}[\mathcal{I}_{\text{FA}-}(x^{\text{S}}, z^{\text{S}})] &\rightarrow \frac{i\Phi_{-1}(x_{\text{s}})}{4N} \left[\frac{1}{N} \sum_{j=1}^N \beta_j \phi_j^2(x^{\text{S}}) e^{i2\beta_j z^{\text{S}}} \right] \\ &\quad - \frac{\omega_0^2 \sigma_{\text{r}} \Phi_{-1}(x_{\text{s}})}{8} \Psi(x^{\text{S}}, -z^{\text{S}}; x_{\text{r}}, z_{\text{r}})^2 + \frac{\omega_0^2 \sigma_{\text{r}} \Phi_{-1}(x_{\text{s}})}{8} \Psi(x^{\text{S}}, -z^{\text{S}}; x_{\text{r}}, -z_{\text{r}})^2, \end{aligned} \quad (5.5)$$

and we find a peak at $z^S = z_r$ and $x^S = x_r$.

Finally we have

$$\Phi_{-1}(x_s) = \frac{2}{aN} \sum_{j=1}^N \beta_j^{-1} \sin^2\left(\frac{2\pi x_s j}{\lambda N}\right) \stackrel{N \gg 1}{\simeq} \frac{1}{a} \int_0^1 \frac{1}{\sqrt{1-x^2}} dx = \frac{\pi}{2a}, \quad (5.6)$$

which completes the proof of the proposition. \square

Remark 5.2. To eliminate the β_j on the denominator, we multiplied by the exact β_j factor in constructing the imaging function. Alternatively, we can differentiate the cross correlation function to remove the denominator; see (4.12). If we do so, the above approximation will lead to the integral

$$\int_{-\frac{\pi}{2}}^{\frac{\pi}{2}} \cos^2 \theta e^{i(\tilde{\eta} \cos \theta + \tilde{\xi} \sin \theta)} d\theta$$

in the square brackets of Eq. (5.3). This function should be compared with (5.7) in the next section.

5.2 The case of limited aperture receiver array

Next, we consider the realistic setting where the receiver array only covers part of the transverse section, namely $\mathcal{A} = (a_1, a_2)$ and $0 < a_1 < a_2 < a$. For a search point (x^S, \tilde{z}^S) , with $\tilde{z}^S = \tilde{L} + z^S$, we have the following result.

Proposition 5.3. *If $a_2 - a_1 \gg \lambda$, $z^S, z_r \gg a$, and $x^S, x_r \in (0, a)$, then*

$$\mathbb{E}[\mathcal{I}_{\text{LA}}(x^S, z^S)] \simeq \frac{\pi \omega_0^2 k^2 \sigma_r (a_2 - a_1)^2}{32a^5} \Re e \left\{ \left[\int_{-\frac{\pi}{2}}^{\frac{\pi}{2}} \cos^2 \theta e^{i(\tilde{\eta} \cos \theta + \tilde{\xi} \sin \theta)} d\theta \right]^2 \right\}, \quad (5.7)$$

where we have introduced the normalized cross range offset $\tilde{\xi} = 2\pi(x_r - x^S)/\lambda$, and the normalized range offset $\tilde{\eta} = 2\pi(z_r - z^S)/\lambda$.

This proposition gives the form of the point spread function of the mean imaging functional, that is the normalized form of the peak centered at the reflector location. The range and cross-range widths of the peak are the range and cross-range resolutions. Since the variables $\tilde{\xi}$ and $\tilde{\eta}$ are normalized with respect to the wavelength, we see that both the range and cross-range resolutions are of order of the wavelength, which is the diffraction limit. The form of the peak can be seen in Figure 2 which plots the transverse and longitudinal shapes of the point spread function

$$h(\tilde{\xi}) = \Re e \left\{ \left[\int_{-\frac{\pi}{2}}^{\frac{\pi}{2}} \cos^2 \theta e^{i\tilde{\xi} \sin \theta} d\theta \right]^2 \right\} = \pi^2 \frac{J_1(\tilde{\xi})^2}{\tilde{\xi}^2}, \quad (5.8)$$

$$g(\tilde{\eta}) = \Re e \left\{ \left[\int_{-\frac{\pi}{2}}^{\frac{\pi}{2}} \cos^2 \theta e^{i\tilde{\eta} \cos \theta} d\theta \right]^2 \right\} = \pi^2 J_1'(\tilde{\eta})^2 - \left[\int_{-\frac{\pi}{2}}^{\frac{\pi}{2}} \cos^2 \theta \sin(\tilde{\eta} \cos \theta) d\theta \right]^2, \quad (5.9)$$

where we have used Formula 9.1.20 [1] to express h and g in terms of the Bessel function J_1 . h and g are even functions maximal at 0 and stationary phase calculations also show that

$$h(\tilde{\xi}) \stackrel{\tilde{\xi} \gg 1}{\simeq} \pi \frac{1 - \sin(2\tilde{\xi})}{\tilde{\xi}^3}, \quad g(\tilde{\eta}) \stackrel{\tilde{\eta} \gg 1}{\simeq} 2\pi \frac{\sin(2\tilde{\eta})}{\tilde{\eta}}.$$

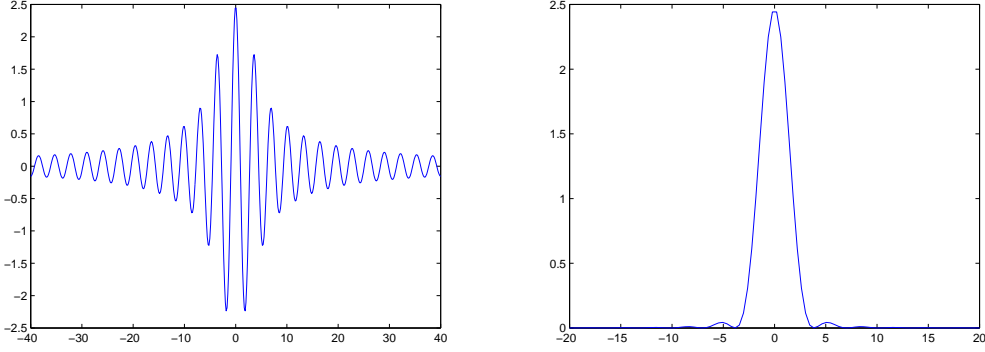


Figure 2: Plots of the functions $g(\tilde{\eta})$ and $h(\tilde{\xi})$ which give the normalized form of the point spread function in the range direction ($g(\tilde{\eta})$, left picture) and in the cross range direction ($h(\tilde{\xi})$, right picture).

Proposition 5.3 also shows that the resolution of the mean imaging functional does not depend on the aperture of the array $a_2 - a_1$. This is a consequence of the waveguide geometry, since multiple reflections at the boundaries of the waveguide generate multiple replicas of the receiver array in the plane $z = \tilde{L}$, which gives an effective aperture that is large enough to reach the diffraction limit.

Proof. Since the two functions above can be analyzed in the same manner, we focus on one of them, namely $\mathcal{I}_{\text{LA}+}$. As before, the cross correlation \mathcal{C} can be treated component-wise. For the function $\mathcal{I}_{\text{LA}+}$, the main contribution comes from the primary-secondary component \mathcal{C}_{ps} , which we focus on for the moment. Let $\mathcal{I}_{+\text{ps}}$ denote this main term, *i.e.*

$$\begin{aligned} \mathcal{I}_{+\text{ps}} &= -\frac{i}{N^2} \int_{\mathcal{A}^2} \sum_{j', q'=1}^N \phi_{q'}(x_1) \phi_{q'}(x_r^s) \phi_{j'}(x_2) \phi_{j'}(x_r^s) \\ &\quad \times (\Delta_{x_1} + k^2)(\Delta_{x_2} + k^2) \mathcal{C}_{\text{ps}}\left(\frac{z^S}{\omega_0}(\beta_{q'} + \beta_{j'}), x_1, x_2\right) dx_1 dx_2. \end{aligned}$$

Then from (5.1) and the fact that $\Delta_{x_1} \phi_j = -\lambda_j^2 \phi_j$ and $k^2 = \lambda_j^2 + \beta_j^2$, we verify that

$$\begin{aligned} \mathbb{E}[\mathcal{I}_{+\text{ps}}] &\longrightarrow \frac{\omega_0^2 \sigma_r \Phi_{-1}(x_s)}{8N^2} \sum_{q, j, q', j'=1}^N \beta_j \beta_q \phi_j(x_r) \phi_{j'}(x^S) \phi_q(x_r) \phi_{q'}(x^S) e^{i(\beta_j + \beta_q)z_r} e^{-i(\beta_{j'} + \beta_{q'})z^S} \\ &\quad \times \int_{\mathcal{A}^2} \phi_j(x_1) \phi_{j'}(x_1) \phi_q(x_2) \phi_{q'}(x_2) dx_1 dx_2. \end{aligned}$$

If $\mathcal{A} = (0, a)$, the last integral will be $\delta_{jj'} \delta_{qq'}$ and we are back in the case of full aperture array. In the current situation, this integral has to be dealt with more carefully. The above limit can be further written as

$$\frac{\omega_0^2 \sigma_r \Phi_{-1}(x_s)}{8} \left[\frac{1}{N} \sum_{j, j'=1}^N \beta_j \phi_j(x_r) \phi_{j'}(x^S) e^{i(\beta_j z_r - \beta_{j'} z^S)} \int_{\mathcal{A}} \phi_j(x_1) \phi_{j'}(x_1) dx_1 \right]^2. \quad (5.10)$$

Introducing the difference index $l = j - j'$, the double sum above can be written in terms of j' and l . The integral over x_1 can be calculated explicitly as follows:

$$\begin{aligned}
\int_{\mathcal{A}} \phi_{j'+l}(x_1) \phi_{j'}(x_1) dx_1 &= \int_{a_1}^{a_2} \frac{2}{a} \sin\left(\frac{(j'+l)\pi x_1}{a}\right) \sin\left(\frac{j'\pi x_1}{a}\right) dx_1 \\
&= \frac{1}{a} \int_{a_1}^{a_2} \cos\left(\frac{\pi l x_1}{a}\right) - \cos\left(\frac{\pi(2j'+l)x_1}{a}\right) dx_1 \\
&= \frac{a_2 - a_1}{a} \left[\cos\left(\frac{\pi l(a_2 + a_1)}{2a}\right) \text{sinc}\left(\frac{\pi l(a_2 - a_1)}{2a}\right) \right. \\
&\quad \left. - \cos\left(\frac{\pi(2j'+l)(a_2 + a_1)}{2a}\right) \text{sinc}\left(\frac{\pi(2j'+l)(a_2 - a_1)}{2a}\right) \right].
\end{aligned}$$

For most j' , the first term above dominates. Hence, the number of indices l 's so that the above quantity is significant is roughly of order $a/(a_2 - a_1)$.

Using the explicit expression $\phi_j(x) = \sqrt{2/a} \sin(j\pi x/a)$, we rewrite the function inside the brackets in (5.10) as

$$\begin{aligned}
\int_{\mathcal{A}} \frac{1}{N} \sum_{j',l} \frac{4\beta_{j'+l}}{a^2} \sin\left(\frac{\pi(j'+l)x_r}{a}\right) \sin\left(\frac{\pi j' x^S}{a}\right) \sin\left(\frac{\pi(j'+l)x_1}{a}\right) \sin\left(\frac{\pi j' x_1}{a}\right) \\
e^{i\beta_{j'}(z_r - z^S)} e^{i(\beta_{j'+l} - \beta_{j'})z_r} dx_1.
\end{aligned}$$

Using the explicit expression $\beta_j = \sqrt{k^2 - (j\pi/a)^2}$ and the fact that the total number of modes N is $\lfloor a/(\lambda/2) \rfloor = \lfloor ak/\pi \rfloor$ and assuming that ak/π is an integer for simplicity, we see that for $l \ll N$,

$$\beta_{j'+l} - \beta_{j'} \approx -\frac{k^2}{\beta_{j'}} \frac{j'}{N} \frac{l}{N}. \quad (5.11)$$

Using this expansion and some trigonometric identities, we approximate the integral above by

$$\begin{aligned}
\int_{\mathcal{A}} \sum_{j',l} \frac{4\beta_{j'+l}}{a^2 N} \left[\sin\left(\frac{\pi j' x_r}{a}\right) \cos\left(\frac{\pi l x_r}{a}\right) + \cos\left(\frac{\pi j' x_r}{a}\right) \sin\left(\frac{\pi l x_r}{a}\right) \right] \sin\left(\frac{\pi j' x^S}{a}\right) e^{-i\frac{k^2}{\beta_{j'}} \frac{j'}{N} \frac{l}{N} z_r} \\
\times \left[\sin^2\left(\frac{\pi j' x_1}{a}\right) \cos\left(\frac{\pi l x_1}{a}\right) + \cos \sin\left(\frac{\pi j' x_1}{a}\right) \sin\left(\frac{\pi l x_1}{a}\right) \right] e^{i2\pi \sqrt{1 - (\frac{j'}{N})^2} \frac{z_r - z^S}{\lambda}} dx_1.
\end{aligned}$$

Defined $\eta = z^S - z_r$ and $\xi = x^S - x_r$. Substitution of some further trigonometric identities transform the above integral into

$$\begin{aligned}
\int_{\mathcal{A}} \frac{1}{a^2 N} \sum_{j',l} \beta_{j'+l} \left\{ \left(\cos\left(\frac{\pi j' \xi}{a}\right) \cos\left(\frac{\pi l x_r}{a}\right) + \sin\left(\frac{\pi j' \xi}{a}\right) \sin\left(\frac{\pi l x_r}{a}\right) \right) \cos\left(\frac{\pi l x_1}{a}\right) + R(j', \xi, l) \right\} \\
e^{i2\pi \sqrt{1 - (\frac{j'}{N})^2} \frac{\eta}{\lambda}} e^{-i \frac{j'/N}{\sqrt{1 - (j'/N)^2}} (\frac{k z_r}{N}) l} dx_1.
\end{aligned} \quad (5.12)$$

Here, $R(j', \xi, l)$ consists of products of trigonometric functions, and for each product, one of the trigonometric functions is evaluated at $\pi j' x_r/a$, $\pi j' x_1/a$ or $\pi j' (x_r + x^S)/a$. Assuming

that x_r/a and x_1/a are of order one, we observe that comparing with $\pi j' \xi/a$, which is explicitly written above and in which ξ can be of order much smaller than one, $\pi j' x_r/a$ varies much faster as j' varies. In other words, $\pi j' x_r/a$ can be viewed as a fast variable, and $\pi j' \xi/a$ with $\xi \ll a$ is a slow variable. Similarly, in the expression of the complex potentials and $\beta_{j'+l}$ for fixed l , the variable j'/N with $N \gg 1$ involved is also a slow variable. Consequently, the contribution of $R(j', \xi, l)$ to the sum over j' is negligible comparing with those of the terms explicitly written. This two-scale analysis also shows that the above integral is much smaller for large ξ comparing with $\xi \ll a$.

We consider the regime $N \gg 1$, and use the continuum approximation to rewrite the sum over j' as an integral with respect to the variable $t = j'/N$. We further assume $1 \ll l \ll N$, which is equivalent to say $a \gg (a_2 - a_1) \gg \lambda$; the second relation validates the linearization (5.11) and allows us replacing $\beta_{j'+l}$ by $\beta_{j'}$, while the first relation justifies the usage of Poisson summation formula

$$\begin{aligned} & \sum_l \cos\left(\frac{\pi l x_r}{a}\right) \cos\left(\frac{\pi l x_1}{a}\right) e^{-i\pi \frac{t}{\sqrt{1-t^2}} \left(\frac{z_r}{a}\right) l} = \frac{\pi}{2} \sum_{m \in \mathbb{Z}} \left[\delta\left(\frac{\pi(x_r + x_1)}{a} - \frac{\pi t}{\sqrt{1-t^2}} \frac{z_r}{a} + 2m\pi\right) \right. \\ & + \delta\left(\frac{\pi(x_r - x_1)}{a} - \frac{\pi t}{\sqrt{1-t^2}} \frac{z_r}{a} + 2m\pi\right) + \delta\left(\frac{\pi(x_r - x_1)}{a} + \frac{\pi t}{\sqrt{1-t^2}} \frac{z_r}{a} + 2m\pi\right) \\ & \left. + \delta\left(\frac{\pi(x_r + x_1)}{a} + \frac{\pi t}{\sqrt{1-t^2}} \frac{z_r}{a} + 2m\pi\right) \right] \end{aligned}$$

and

$$\begin{aligned} & \sum_l \sin\left(\frac{\pi l x_r}{a}\right) \cos\left(\frac{\pi l x_1}{a}\right) e^{-i\pi \frac{t}{\sqrt{1-t^2}} \left(\frac{z_r}{a}\right) l} = \frac{\pi}{2i} \sum_{m \in \mathbb{Z}} \left[\delta\left(\frac{\pi(x_r + x_1)}{a} - \frac{\pi t}{\sqrt{1-t^2}} \frac{z_r}{a} + 2m\pi\right) \right. \\ & + \delta\left(\frac{\pi(x_r - x_1)}{a} - \frac{\pi t}{\sqrt{1-t^2}} \frac{z_r}{a} + 2m\pi\right) - \delta\left(\frac{\pi(x_r - x_1)}{a} + \frac{\pi t}{\sqrt{1-t^2}} \frac{z_r}{a} + 2m\pi\right) \\ & \left. - \delta\left(\frac{\pi(x_r + x_1)}{a} + \frac{\pi t}{\sqrt{1-t^2}} \frac{z_r}{a} + 2m\pi\right) \right] \end{aligned}$$

Note that we have used the fact that $k/N = \pi/a$ again. For each fixed m , let $\delta_\alpha(x_1, x_r; z_r, m)$, $\alpha = 1, \dots, 4$, denote the four Dirac distributions. Define also $\tilde{\eta} = 2\pi\eta/\lambda$, $\tilde{\xi} = 2\pi\xi/\lambda$; Then we have $\cos(\pi j' \xi/a) = \cos(\tilde{\xi}t)$; the integral above becomes

$$\begin{aligned} & \frac{k\pi}{2a^2} \int_0^1 \sqrt{1-t^2} \left[\int_{\mathcal{A}} e^{i(\sqrt{1-t^2}\tilde{\eta}-t\tilde{\xi})} \sum_{m \in \mathbb{Z}} (\delta_1 + \delta_2)(x_1, x_r; z_r, m) \right. \\ & \left. + e^{i(\sqrt{1-t^2}\tilde{\eta}+t\tilde{\xi})} \sum_{m \in \mathbb{Z}} (\delta_3 + \delta_4)(x_1, x_r; z_r, m) dx_1 \right] dt. \end{aligned}$$

If we extend the domain of t to $(-1, 1)$, the above integral simplifies to

$$\frac{k\pi}{2a^2} \int_{-1}^1 \sqrt{1-t^2} \left[\int_{\mathcal{A}} e^{i(\sqrt{1-t^2}\tilde{\eta}+t\tilde{\xi})} \sum_{m \in \mathbb{Z}} (\delta_3 + \delta_4)(x_1, x_r; z_r, m) \right] dt.$$

Integrate over x_1 first. The two Dirac distributions restrict the range of integration of t to

the following intervals respectively:

$$\frac{(a_1 + 2ma) - x_r}{z_r} \leq \frac{t}{\sqrt{1-t^2}} \leq \frac{(a_2 + 2ma) - x_r}{z_r},$$

$$\frac{(-a_2 + 2ma) - x_r}{z_r} \leq \frac{t}{\sqrt{1-t^2}} \leq \frac{(-a_1 + 2ma) - x_r}{z_r}.$$

To interpret these conditions, imagine that the boundaries of the waveguide are two mirrors, then the array (a_1, a_2) has an image $(-a_2, -a_1)$ in the lower mirror; the two mirrors then generate a replica of images $(a_1 + 2ma, a_2 + 2ma)$ and $(-a_2 + 2ma, -a_1 + 2ma)$. If we define an angle θ by

$$\theta = \arctan \frac{t}{\sqrt{1-t^2}}, \quad t \in (-1, 1),$$

then the above restrictions of the Dirac measures can be restated as

$$\arctan \frac{x_r + a_1 + 2ma}{z_r} \leq \theta \leq \arctan \frac{x_r + a_2 + 2ma}{z_r},$$

$$\arctan \frac{x_r - a_2 + 2ma}{z_r} \leq \theta \leq \arctan \frac{x_r - a_1 + 2ma}{z_r}.$$

The first one restrict the angle θ to those formed by the reflector and the array (a_1, a_2) and the images of this array. The second set restrict the angle θ to those formed by the reflector and the image array $(-a_2, -a_1)$ and the replicas.

To analyze the resulting integral, we consider the simplest set-up where: (a_1, a_2) is centered in the cross section; the reflector is also centered in the cross range direction, *i.e.* $x_r = a/2$. Further we assume the large distance regime $z_r \gg a$.

In such a setting, with the notation $a_c = (a_1 + a_2)/2$ and $w = (a_2 - a_1)/2$, the integral above boils down to

$$\frac{k}{2a} \sum_{m \in \mathbb{Z}} \int_{\arctan(ma+a_c-w-x_r)/z_r}^{\arctan(ma+a_c+w-x_r)/z_r} \cos^2 \theta e^{i(\tilde{\eta} \cos \theta + \tilde{\xi} \sin \theta)} d\theta.$$

Since $w \ll z_r$, for each fixed m , the integral is over a very small angle section. Hence we can approximate the integral by the value at mean angle times the length of the angle section. The mean angle θ_m in the angle section is $\arctan ma/z_r$. We further check that $\cos \theta_m = 1/\sqrt{1 + (ma/z_r)^2}$. Consequently, with a/z_r set to Δx , the sum becomes

$$\frac{k}{2a} \frac{2w}{z_r} \frac{z_r}{a} \sum_{m=-\infty}^{\infty} \frac{\exp\{i(\tilde{\eta} + m\Delta x \tilde{\xi})(\sqrt{1 + (m\Delta x)^2})^{-1}\}}{(1 + (m\Delta x)^2)^2} \Delta x$$

$$\approx \frac{k}{2a} \frac{a_2 - a_1}{a} \int_{-\infty}^{\infty} \frac{e^{i\tilde{\eta}/\sqrt{1+x^2} + i\tilde{\xi}x/\sqrt{1+x^2}}}{(1+x^2)^2} dx = \frac{k}{2a} \frac{a_2 - a_1}{a} \int_{-\pi/2}^{\pi/2} \cos^2 \theta e^{i\tilde{\eta} \cos \theta + i\tilde{\xi} \sin \theta} d\theta.$$

Finally, let us verify that the primary-primary and secondary-primary cross correlations do not have significant contributions to the imaging functional \mathcal{I}_{LA+} . Let \mathcal{I}_{+pp} and \mathcal{I}_{+sp} denote these two terms respectively. Similar to (5.10), the expectation of \mathcal{I}_{+sp} converges, as $\varepsilon \rightarrow 0$, to

$$-\frac{\omega_0^2 \sigma_r \Phi_{-1}(x_s)}{8} \left[\frac{1}{N} \sum_{j,j'=1}^N \beta_j \phi_j(x_r) \phi_{j'}(x^S) e^{-i(\beta_j z_r + \beta_{j'} z^S)} \int_{\mathcal{A}} \phi_j(x_1) \phi_{j'}(x_1) dx_1 \right]^2. \quad (5.13)$$

This function has the same form of (5.10) and can be analyzed in the same way. The key of these two functions is that the phase function in $\mathcal{I}_{+\text{sp}}$ is a sum. As a result, the variable η in (5.12) cannot be defined and have to be replaced by $z_r + z^S$ which is of order a . This renders $e^{i2\pi\sqrt{1-(j'/N)^2}(z_r+z^S)/\lambda}$ fast varying no matter how close z^S is to z_r . Due to the averaging of fast oscillations, there is no significant contribution from $\mathcal{I}_{+\text{sp}}$.

For the primary-primary component, the analog to (5.10) reads

$$\mathbb{E}[\mathcal{I}_{+\text{pp}}] \longrightarrow \frac{-i\Phi_{-1}(x_s)}{2a} \sum_j \beta_j^3 \left[\int_{\mathcal{A}} \phi_j(x_1) \frac{1}{N} \sum_{j'} \sin\left(\frac{2\pi x_1}{\lambda} \frac{j}{N}\right) e^{-2\pi\sqrt{1-(j'/N)^2} \frac{z^S}{\lambda}} dx_1 \right]^2. \quad (5.14)$$

Again, in the sum over j' , only fast variables are involved. In the regime $N \gg 1$, the contribution of the function above is negligible.

The term $\mathcal{I}_{\text{LA}-}$ can be analyzed similarly. Combining the main contributions in $\mathcal{I}_{\text{LA}+}$ and $\mathcal{I}_{\text{LA}-}$, we obtain the desired result. \square

5.3 Imaging with Broadband Sources

As we will see in Section 6, the imaging functionals are not statistical stable if the source is time-harmonic. Hence it is required to consider a broadband source (4.6). We show that the results obtained above for the means of imaging functionals apply to the broadband setting as well.

Using Proposition 3.1, the main contribution of the two moment of mode coupling matrix at the same frequency comes from the case when $j = m$ and $l = n$. Therefore,

$$\mathbb{E} \varepsilon^\alpha \mathcal{C}_{\text{pp}}(\tau, x_1, x_2) \longrightarrow \frac{\Phi_{-1}(x_s)}{4} \sum_{j=1}^N \frac{\phi_j(x_1)\phi_j(x_2)}{\beta_j} \lim_{\varepsilon \rightarrow 0} e^{-i\omega_0\tau} \frac{1}{2\pi} \int |\hat{f}_0(h)|^2 e^{-i\varepsilon^\alpha \tau h} dh.$$

Similarly, for the primary-secondary field, we have

$$\begin{aligned} \mathbb{E} \varepsilon^\alpha \mathcal{C}_{\text{ps}}(\tau, x_1, x_2) &\longrightarrow \frac{i\omega_0^2 \Phi_{-1}(x_s) \sigma_r}{8} \sum_{q,j=1}^N \frac{\phi_j(x_1)\phi_j(x_r)\phi_q(x_2)\phi_q(x_r)}{\beta_q\beta_j} \\ &\quad \times \lim_{\varepsilon \rightarrow 0} e^{i(\beta_q+\beta_j)z_r} e^{-i\omega_0\tau} \frac{1}{2\pi} \int |\hat{f}_0(h)|^2 e^{i(\beta'_q+\beta'_j)\varepsilon^\alpha h z_r} e^{-i\varepsilon^\alpha h \tau} dh. \end{aligned}$$

For the secondary-primary field, we have

$$\begin{aligned} \mathbb{E} \varepsilon^\alpha \mathcal{C}_{\text{ps}}(\tau, x_1, x_2) &\longrightarrow \frac{-i\omega_0^2 \Phi_{-1}(x_s) \sigma_r}{8} \sum_{q,j=1}^N \frac{\phi_q(x_1)\phi_q(x_r)\phi_j(x_2)\phi_j(x_r)}{\beta_q\beta_j} \\ &\quad \times \lim_{\varepsilon \rightarrow 0} e^{-i(\beta_q+\beta_j)z_r} e^{-i\omega_0\tau} \frac{1}{2\pi} \int |\hat{f}_0(h)|^2 e^{-i(\beta'_q+\beta'_j)\varepsilon^\alpha h z_r} e^{-i\varepsilon^\alpha h \tau} dh. \end{aligned}$$

From these limits, we see that as long as z_r , the distance between the reflector and the array is much smaller than $\varepsilon^{-\alpha}$, the integral in h above can be approximated by the energy of the source (square L^2 norm of f_0). The rest parts of the limiting expectation of the cross correlation functions are exactly the same as the time-harmonic case. Consequently, the resolution analyses in the previous subsections based on the mean value of the cross-correlation migration imaging functionals remain the same.

6 Stability Analysis of the Imaging Functionals

The key tool is the following proposition which analyzes the asymptotic behavior of the fourth-order moment of the transmission coefficients in the limit $\varepsilon \rightarrow 0$; see [10, Section 20.9.3] or [11, Section 8.4].

Proposition 6.1. *The expectation of four transmission coefficients at the same frequency has a limit as $\varepsilon \rightarrow 0$. In the regime $L \gg L_{\text{equip}}$ we have*

$$\lim_{\varepsilon \rightarrow 0} \mathbb{E}[\overline{T_{jl}^\varepsilon T_{mn}^\varepsilon} \overline{T_{j'l'}^\varepsilon T_{m'n'}^\varepsilon}] \stackrel{L \gg L_{\text{equip}}}{\simeq} \begin{cases} \frac{2}{N(N+1)} & \text{if } (j, l) = (m, n) = (j', l') = (m', n'), \\ \frac{1}{N(N+1)} & \text{if } (j, l) = (m, n) \neq (j', l') = (m', n'), \\ \frac{1}{N(N+1)} & \text{if } (j, l) = (m', n') \neq (j', l') = (m, n), \\ 0 & \text{otherwise.} \end{cases}$$

Let $\alpha \in (0, 2)$ and $h \neq 0$. The expectation of four transmission coefficients at two frequencies ω and $\omega + \varepsilon^\alpha h$ has a limit as $\varepsilon \rightarrow 0$. In the regime $L \gg L_{\text{equip}}$ we have

$$\lim_{\varepsilon \rightarrow 0} \mathbb{E}[\overline{T_{jl}^\varepsilon T_{mn}^\varepsilon}(\omega) \overline{T_{j'l'}^\varepsilon T_{m'n'}^\varepsilon}(\omega + \varepsilon^\alpha h)] \stackrel{L \gg L_{\text{equip}}}{\simeq} \begin{cases} \frac{1}{N^2} & \text{if } (j, l) = (m, n) \text{ and } (j', l') = (m', n'), \\ 0 & \text{otherwise.} \end{cases}$$

The previous section shows that the mean of the imaging functional has a peak centered at the reflector location. The width of the peak is of the order of the wavelength. However, the imaging functional will give the reflector location only if it is statistically stable, that is to say, if the standard deviation of the fluctuations of the imaging functional is smaller than the mean amplitude of the peak.

6.1 Time-harmonic case

We address the full aperture case in which the imaging functional is defined by (4.10). By using (5.4-5.5) the mean of the imaging functional is

$$\mathbb{E}[\mathcal{I}_{\text{FA}}(x^{\text{S}}, z^{\text{S}})] = \frac{\omega_0^2 \sigma_{\text{r}}}{4} \Phi_{-1}(x_{\text{s}}) \left\{ \Re e(\Psi(x^{\text{S}}, z^{\text{S}}; x_{\text{r}}, z_{\text{r}})^2) + O\left(\frac{1}{kz^{\text{S}}}\right) + O\left(\frac{1}{N\omega_0^2 \sigma_{\text{r}}}\right) \right\}, \quad (6.1)$$

where Φ_j and Ψ are defined by (3.14) and (3.15). Here:

- The term with the real part comes from the contributions of the cross correlation of secondary (reflected) and primary waves \mathcal{C}_{ps} and \mathcal{C}_{sp} that contain $\Psi(x^{\text{S}}, z^{\text{S}}; x_{\text{r}}, z_{\text{r}})$ (second term in (5.4)) or $\Psi(x^{\text{S}}, -z^{\text{S}}; x_{\text{r}}, -z_{\text{r}})$ (third term in (5.5)).
- The term $O(1/(kz^{\text{S}}))$ comes from the contributions of the cross correlation of secondary (reflected) and primary waves \mathcal{C}_{ps} and \mathcal{C}_{sp} that contain $\Psi(x^{\text{S}}, -z^{\text{S}}; x_{\text{r}}, z_{\text{r}})$ or $\Psi(x^{\text{S}}, z^{\text{S}}; x_{\text{r}}, -z_{\text{r}})$ (third term in (5.4) and second term in (5.5)). In such a case there are at least a product of two these terms, which gives the $1/(kz^{\text{S}})$ decay.
- The term $O(1/(N\omega_0^2 \sigma_{\text{r}}))$ comes the contributions of the cross correlation of primary waves \mathcal{C}_{pp} (the first terms in (5.4) and in (5.5)).

The expression (6.1) is valid provided N is large enough so that $N\omega_0^2 \sigma_{\text{r}} \gg 1$. Then it is true that the mean imaging functional is dominated by the first term in the right hand

side, which is a peak centered at the reflector location. The mean amplitude of the peak at the reflector location is

$$P_{\text{peak}} = \frac{\omega_0^2 \sigma_r}{4} \Phi_{-1}(x_s) \Phi_0(x_r)^2.$$

In the continuum approximation $N \gg 1$, we have (5.6) and

$$\Phi_0(x_r) = \frac{2}{aN} \sum_{j=1}^N \sin^2\left(\frac{2\pi x_r j}{\lambda N}\right) \stackrel{N \gg 1}{\simeq} \frac{1}{a}, \quad (6.2)$$

and therefore

$$P_{\text{peak}} = \frac{\pi \omega_0^2 \sigma_r}{8a^3}. \quad (6.3)$$

The second moment of the imaging functional can be computed using Proposition 6.1 in the regime $\varepsilon \ll 1$ and $L \gg L_{\text{equip}}$.

$$\begin{aligned} \mathbb{E}[|\mathcal{I}_{\text{FA}}(x^S, z^S)|^2] &= \frac{N}{N+1} |\mathbb{E}[\mathcal{I}_{\text{FA}}(x^S, z^S)]|^2 \\ &\quad + \frac{\omega_0^4 \sigma_r^2 N}{32(N+1)} \Phi_{-1}^2(x_s) \left\{ \Phi_1(x^S) \Phi_{-1}(x_r) |\Psi(x^S, z^S; x_r, z_r)|^2 \right. \\ &\quad \left. + \Re(\Psi(x^S, z^S; x_r, z_r)^4) + O\left(\frac{1}{kz^S}\right) + O\left(\frac{1}{N^2 \omega_0^4 \sigma_r^2}\right) \right\}. \quad (6.4) \end{aligned}$$

Here:

- The term $O(1/(kz^S))$ comes from the contributions of the cross correlation of secondary (reflected) and primary waves \mathcal{C}_{ps} and \mathcal{C}_{sp} that contain $\Psi(x^S, -z^S; x_r, z_r)$ or $\Psi(x^S, z^S; x_r, -z_r)$ (in such a case there are at least a product of two these terms, which gives the $1/(kz^S)$ decay).
- The term $O(1/(N\omega_0^2\sigma_r)^2)$ comes from the contribution of the cross correlation of primary waves \mathcal{C}_{pp} that can be computed in a more quantitative way:

$$O\left(\frac{1}{N^2 \omega_0^4 \sigma_r^2}\right) = \frac{4}{N^2 \omega_0^4 \sigma_r^2} \Phi_1(x^S)^2 + o\left(\frac{1}{N^2 \omega_0^4 \sigma_r^2}\right).$$

The variance of the imaging functional at the reflector location is therefore

$$\text{Var}(\mathcal{I}_{\text{FA}}(x_r, z_r)) = P_{\text{peak}}^2 \left\{ \frac{1}{2} + \frac{1}{2} \frac{\Phi_1(x_r) \Phi_{-1}(x_r)}{\Phi_0^2(x_r)} + O\left(\frac{1}{kz^S}\right) + O\left(\frac{1}{N^2 \omega_0^4 \sigma_r^2}\right) \right\}.$$

In the continuum approximation $N \gg 1$, we have (5.6), (6.2), and

$$\Phi_1(x_r) = \frac{2}{aN} \sum_{j=1}^N \beta_j \sin^2\left(\frac{2\pi x_r j}{\lambda N}\right) \stackrel{N \gg 1}{\simeq} \frac{1}{a} \int_0^1 \sqrt{1-x^2} dx = \frac{\pi}{4a}, \quad (6.5)$$

and therefore

$$\text{Var}(\mathcal{I}_{\text{FA}}(x_r, z_r)) = P_{\text{peak}}^2 \left\{ \frac{1}{2} + \frac{1}{2} \frac{\pi^2}{8} \right\}. \quad (6.6)$$

To summarize:

- 1) The typical amplitude of the fluctuations of the imaging functional for $(x^S, z^S) = (x_r, z_r)$

(i.e. at the reflector location) is P_{peak} (as shown by (6.6)).

2) The typical amplitude of the fluctuations of the imaging functional for $|(x^S, z^S) - (x_r, z_r)| \gg \lambda_0$ (i.e. away from the reflector location) is $P_{\text{peak}}((\lambda_0/|z^S - z_r|)^{1/2} \wedge (\lambda_0|x^S - x_r|)^{3/2} + \lambda_0^2/(N\sigma_r))$ (as shown by (6.4)).

The second result shows that the fluctuations of the image far from the main peak location are of the order of $\lambda_0^2/(N\sigma_r)$ relatively to the amplitude of the main peak. They are due to the contributions of the primary cross correlation. Provided the number of modes is large enough $N \gg \lambda_0^2/\sigma_r$, they are small.

The first result shows that the amplitude of the peak at the reflector location has relative fluctuations of order one. This is due to the fact that the reflector is illuminated by a field whose amplitude is randomly spatially varying, so that the reflected energy is proportional to the squared amplitude of the primary field at the reflector location, which is a random quantity. This is the origin of the statistical instability in the time-harmonic case.

6.2 Broadband case

We know that the frequency coherence radius Ω_c in a waveguide with length L/ε^2 is of the order of ε^2 (see [10, Proposition 20.7] or [11, Proposition 6.3]). As a result, as soon as a broadband source with a bandwidth larger than Ω_c is used, then the field is the superposition of decorrelated frequency components. As a consequence the field is self-averaging in the time domain.

More exactly, from the expressions of the cross correlations in the broadband case given in Subsection 4.1.1, the mean and the variance of the imaging functional are of the form

$$\begin{aligned} \mathbb{E}[\mathcal{I}_{\text{FA}}(x^S, z^S)] &= \int dh |\hat{f}_0(h)|^2 \sum_{j,l,m,n} \mathbb{E}[\overline{T_{jl}^\varepsilon} T_{mn}^\varepsilon(\omega_0 + \varepsilon^\alpha h)] c_{j,l,m,n}(x^S, z^S), \\ \text{Var}(\mathcal{I}_{\text{FA}}(x^S, z^S)) &= \iint dh dh' |\hat{f}_0(h)|^2 |\hat{f}_0(h')|^2 \sum_{j,l,m,n,j',l',m',n'} \\ &\quad \left\{ \mathbb{E}[\overline{T_{jl}^\varepsilon} T_{mn}^\varepsilon(\omega_0 + \varepsilon^\alpha h) T_{j'l'}^\varepsilon \overline{T_{m'n'}^\varepsilon}(\omega_0 + \varepsilon^\alpha h')] \right. \\ &\quad \left. - \mathbb{E}[\overline{T_{jl}^\varepsilon} T_{mn}^\varepsilon(\omega_0 + \varepsilon^\alpha h)] \mathbb{E}[T_{j'l'}^\varepsilon \overline{T_{m'n'}^\varepsilon}(\omega_0 + \varepsilon^\alpha h')] \right\} c_{j,l,m,n}(x^S, z^S) \overline{c_{j',l',m',n'}(x^S, z^S)}, \end{aligned}$$

where $c_{j,l,m,n}(x^S, z^S)$ is a shorthand for the deterministic coefficient that contains the phase and mode amplitudes.

First, since $\mathbb{E}[\overline{T_{jl}^\varepsilon} T_{mn}^\varepsilon(\omega_0 + \varepsilon^\alpha h)]$ is independent on h to leading order (because $\alpha > 0$), the mean satisfies

$$\mathbb{E}[\mathcal{I}_{\text{FA}}(x^S, z^S)]_{\text{broadband}} \sim \mathbb{E}[\mathcal{I}_{\text{FA}}(x^S, z^S)]_{\text{narrowband}}$$

as already noticed.

Second, the term in the curly brackets in the expression of the variance is vanishing if $\varepsilon^\alpha |h - h'|$ is larger than the frequency coherence radius Ω_c . So the double integral in (h, h') is reduced to a domain that has the form of a thin diagonal band, whose thickness is limited

by the frequency coherence radius Ω_c . As a result we obtain that

$$\begin{aligned} \text{Var}(\mathcal{I}_{\text{FA}}(x^{\text{S}}, z^{\text{S}})) &\sim \iint_{\varepsilon^\alpha |h-h'| \leq \Omega_c} dh dh' |\hat{f}_0(h)|^2 |\hat{f}_0(h')|^2 \sum_{j,l,m,n,j',l',m',n'} \\ &\quad \left\{ \mathbb{E} [\overline{T_{jl}^\varepsilon T_{mn}^\varepsilon}(\omega_0) T_{j'l'}^\varepsilon \overline{T_{m'n'}^\varepsilon}(\omega_0)] \right. \\ &\quad \left. - \mathbb{E} [\overline{T_{jl}^\varepsilon} T_{mn}^\varepsilon(\omega_0)] \mathbb{E} [T_{j'l'}^\varepsilon \overline{T_{m'n'}^\varepsilon}(\omega_0)] \right\} c_{j,l,m,n}(x^{\text{S}}, z^{\text{S}}) \overline{c_{j',l',m',n'}(x^{\text{S}}, z^{\text{S}})}, \end{aligned}$$

or more simply

$$\text{Var}(\mathcal{I}_{\text{FA}}(x^{\text{S}}, z^{\text{S}}))_{\text{broadband}} \sim \text{Var}(\mathcal{I}_{\text{FA}}(x^{\text{S}}, z^{\text{S}}))_{\text{narrowband}} \frac{\Omega_c}{B},$$

where $B \sim \varepsilon^\alpha$ is the bandwidth of the source that is larger than the frequency coherence radius $\Omega_c \sim \varepsilon^2$. We had seen that the use of broadband sources does not affect the resolution of the imaging functional but it ensures its statistical stability. Provided the bandwidth is larger than the frequency coherence radius, the typical amplitude of the fluctuations of the imaging functional is smaller than the amplitude P_{peak} of the main peak at the reflector location, and therefore the reflector can be localized.

7 Conclusions

In this paper we have shown that migration of the cross correlations of the data recorded by a passive receiver array can allow for diffraction-limited imaging of the reflector in a random waveguide even though the sources are very far from the reflector, provided the receivers are close enough from it. The statistical stability of the imaging functional is ensured by the use of broadband sources. The resolution properties are ensured by the waveguide geometry: even when the receiver array does not span the whole cross section of the waveguide, the width of the point spread function of the imaging functional is of the order of the wavelength, provided the diameter of the array is larger than the wavelength.

This paper has addressed the case of a two-dimensional waveguide with Dirichlet boundary conditions, but the conclusions should be qualitatively the same for fairly general situations, when addressing three-dimensional waveguides, with Neumann, Dirichlet or mixed boundary conditions, with random fluctuations of the index of refraction or of the boundaries as in [2, 15].

Acknowledgements

The authors would like to thank the anonymous referees for their careful reading of the manuscript and helpful comments. This work was supported by ERC Advanced Grant Project MULTIMOD-267184.

References

- [1] M. Abramowitz and I. Stegun (editors), *Handbook of Mathematical Functions*, National Bureau of Standards, Washington D.C., 1964.

- [2] R. Alonso, L. Borcea, and J. Garnier, Wave propagation in waveguides with rough boundaries, *Communications in Mathematical Sciences*, **11** (2012), pp. 233-267.
- [3] A. Bakulin and R. Calvert, The virtual source method: Theory and case study, *Geophysics*, **71** (2006), pp. SI139-SI150.
- [4] L. Borcea, J. Garnier, G. Papanicolaou, and C. Tsogka, Coherent interferometric imaging, time gating, and beamforming, *Inverse Problems*, **27** (2011), 065008.
- [5] L. Borcea, J. Garnier, G. Papanicolaou, and C. Tsogka, Enhanced statistical stability in coherent interferometric imaging, *Inverse Problems*, **27** (2011), 085004.
- [6] L. Borcea, G. Papanicolaou, and C. Tsogka, Interferometric array imaging in clutter, *Inverse Problems*, **21** (2005), pp. 1419-1460.
- [7] L. Borcea, G. Papanicolaou, and C. Tsogka, Adaptive interferometric imaging in clutter and optimal illumination, *Inverse Problems*, **22** (2006), pp. 1405-1436.
- [8] L. Borcea, G. Papanicolaou, and C. Tsogka, Coherent interferometric imaging in clutter, *Geophysics*, **71** (2006), pp. SI165-SI175.
- [9] A. Curtis, P. Gerstoft, H. Sato, R. Snieder, and K. Wapenaar, Seismic interferometry - turning noise into signal, *The Leading Edge*, **25** (2006), pp. 1082-1092.
- [10] J.-P. Fouque, J. Garnier, G. Papanicolaou, and K. Sølna, *Wave propagation and time reversal in randomly layered media*, Springer, New York, 2007.
- [11] J. Garnier and G. Papanicolaou, Pulse propagation and time reversal in random waveguides, *SIAM J. Appl. Math.*, **67** (2007), pp. 1718-1739.
- [12] J. Garnier and G. Papanicolaou, Passive sensor imaging using cross correlations of noisy signals in a scattering medium, *SIAM J. Imaging Sci.*, **2** (2009), pp. 396-437.
- [13] J. Garnier and G. Papanicolaou, Resolution analysis for imaging with noise, *Inverse Problems*, **26** (2010), 074001.
- [14] J. Garnier and G. Papanicolaou, Correlation based virtual source imaging in strongly scattering random media, *Inverse Problems*, **28** (2012), 075002.
- [15] C. Gomez, Wave propagation in shallow-water random waveguides, *Commun. Math. Sci.*, **9** (2011), pp. 81-125.
- [16] K. G. Sabra, P. Gerstoft, P. Roux, and W. Kuperman Surface wave tomography from microseisms in Southern California, *Geophys. Res. Lett.*, **32** (2005), L14311.
- [17] G. T. Schuster, *Seismic Interferometry*, Cambridge University Press, Cambridge, 2009.
- [18] K. Wapenaar, E. Slob, R. Snieder, and A. Curtis, Tutorial on seismic interferometry: Part 2 - Underlying theory and new advances, *Geophysics*, **75** (2010), pp. 75A211-75A227.